TURBULENCE MEASUREMENTS IN A COMPLEX FLOWFIELD USING A SIX-ORIENTATION HOT-WIRE PROBE TECHINIQUE

By

SALIM IQBAL JANJUA

Bachelor of Science
University of Punjab
Pakistan
1971

Bachelor of Engineering
Concordia University
Montreal, Canada
1980

Submitted to the Faculty of the Graduate College
of the Oklahoma State University
in partial fulfillment of the requirements
for the Degree of
MASTER OF SCIENCE
December, 1981

TURBULENCE MEASUREMENTS IN A COMPLEX
FLOWFIELD USING A SIX-ORIENTATION
HOT-WIRE PROBE TECHNIQUE

Thesis Approved:

Dennis G. Lilley
Thesis Adviser

Troy D. Reed

Norman N. Durham
Dean of the Graduate College

ACKNOWLEDGMENTS

The author wishes to express his appreciation to his major adviser, Dr. David G. Lilley for his advice and guidance concerning this work. Gratitude is also extended to other committee members, Dr. John A. Wiebelt and Dr. Troy D. Reed.

Further appreciation is extended to Dr. Dennis K. McLaughlin for his great help and useful advice during major part of this study.

The author also wishes to thank Mrs. Camille Tindall for her expert typing skills and advice in the preparation of this thesis.

Finally, the author recognizes the financial support of National Aeronautics and Space Administration through Grant No. NAG3-74, 1980.

TABLE OF CONTENTS

LIST OF TABLES

LIST OF FIGURES

NOMENCLATURE

A, B, C	Calibration constants in Equation 1
AO, BO, CO	Cooling velocity functions in Table I
D	Test section diameter
d	Inlet nozzle diameter
E	Hot-wire voltage
F1	Velocity function for axial velocity
F2	Velocity function for azimuthal velocity
F3	Velocity function for radial velocity
G	Pitch factor
K	Yaw factor
$K_{z_P z_Q}$	Covariance for cooling velocities Z_P, and Z_Q
P, Q, R	Selected hot-wire probe positions
T	Matrix given in Table II, Appendix A
u	Axial velocity
v	Radial velocity
w	Azimuthal (swirl) velocity
$\hat{u}$, $\hat{w}$, $\hat{v}$	Probe coordinate system defined by Figure 6, Appendix B
x, r, θ	Axial, radial, azimuthal cylindrical polar coordinates
Z	Effective cooling velocity acting on a wire
α	Side-wall expansion angle

σ^2	Variance of a given quantity
π	Function defined by Equation 31, 32, and 33
ϕ	Inverse function of calibration equation
ρ	Function of selected mean effective cooling velocities given by Equations 34 through 36

Subscripts

1, 2, 3, 4, 5, 6	Refer to the six probe measuring positions
i, j, P, Q, R	Refer to the three selected cooling velocities
rms	Root-mean-squared quantity

Superscripts

$\overline{}$	Time mean average
$'$	Fluctuating quantity

CHAPTER I

INTRODUCTION

1.1 The Combustor Flowfield Investigation

Understanding the fluid dynamics of the flow in a gas turbine combustion chamber has been of great concern to designers in recent years. A gas turbine combustor, shown in Figure 1, Appendix B, must burn fuel completely, cause little pressure drop, produce gases of nearly uniform temperature, occupy small volume, and maintain stable combustion over a wide range of operating conditions. The designer has a formidable problem in aerothermochemistry, and more thorough and accurate procedures can help in accomplishing the design objectives more quickly and less expensively in the near future.

Intensive research is being carried out at Oklahoma State University on the subject of gas turbine flowfield investigations in the absence of combustion. Figure 2, Appendix B, shows the characteristics of the simplified flowfield being investigated. Flow enters through a jet of diameter d into a tube of diameter D, after being expanded through an angle α. Before entering the tube, the flow may be swirled by a swirler located upstream of the inlet plane. The flowfield is presently being investigated using various methods of approach, such as computer modeling of the flowfield and flow visualization for both swirl and nonswirl conditions (2, 3).

1.2 Previous Experimental Studies on Expansion Flows

Several studies on time-mean flowfields of the type just described have been carried out using various turbulence measuring techniques (4-11). Unfortunately, most of the techniques used do not give complete and detailed information about the flow in terms of all its time-mean and turbulence quantities. There is a strong need to obtain all the turbulence quantities in a complex flowfield using a minimum amount of instrumentation and without causing a great deal of interference with the flow.

1.3 The Turbulence Measurement Problem

Turbulence measurement in a complex flowfield has always been a complicated problem encountered by engineers. In the past, turbulence phenomena have been discussed by various authors in detail and various methods of turbulence measurement have been suggested (12-15). One of the most widely used instruments to obtain turbulence quantities is the hot-wire anemometer. The most common of all hot-wire anemometers is a single hot-wire. When used at a single orientation and in a two-dimensional flow, a single hot-wire can measure the streamwise components of the time-mean velocity and the root-mean-square velocity fluctuation at a particular location in the flowfield. A two-wire probe can be used to determine the time-mean velocities, streamwise and cross stream turbulence intensities, and the cross correlation between the two components of the velocity fluctuations (16-18). To measure the three velocities and their corresponding fluctuating components in a three-dimensional flowfields such as encountered in combustor simulators, there are two methods that can be employed at a point in the flowfield:

1. A multi-wire probe used with a single orientation.
2. A single-wire probe used with a multi-orientation.

Multi-wire techniques, with three hot-wires mounted on the same base so that they all lie within the same volume of the flowfield, permit the necessary three sets of readings to be made simultaneously. The requirement is to determine all three components simultaneously. The main disadvantages of such a technique are:

i. It requires three closely matched anemometer units.
ii. The probes interfere with each other unless they are carefully placed relative to the time-mean velocity vector.
iii. The spatial resolution is poor because of the large size of the probe assembly.
iv. Heat can be convected from one wire to another giving biased readings.

Multi-orientation of a single hot-wire is a novel way to measure the three components of a velocity vector and their fluctuating components. A method devised by Dvorak and Syred (19) uses a single normal hot-wire oriented at three different positions such that the center one is separated by 45 degrees from the other two. The velocity vector at a location is related to the three orthogonal components using pitch and yaw factors as defined by Jorgensen (20). The data are obtained in the form of mean and root-mean-square voltages at each orientation. However, the measurements done with a single wire do not supply all the information needed to obtain the turbulence quantities. Therefore in addition to a single wire, Dvorak and Syred used a cross-wire probe to obtain the covariances between the voltages obtained at adjacent hot-wire orientations. A cross-wire probe, two wires mounted on the same base and separated by 45 degrees from each other, poses the same problems as already discussed for a multi-wire probe.

King (21) modified the technique developed by Dvorak and Syred. His method calls for a normal hot-wire to be oriented through six different positions, each orientation separated by 30 degrees from the adjacent one. Thus, one measures mean and root-mean-square voltages at each orientation. The data reduction is done using some assumptions regarding the statistical nature of turbulence, making it possible to solve for the three time-mean velocities, the three normal turbulent stresses, and the three turbulent sheer stresses. Having obtained these quantities, one can in addition calculate the kinetic energy of turbulence. Various recent studies discuss the turbulence measurement problem, with emphasis on hot-wire and laser anemometer applications to swirl flows (22-23).

1.4 The Scope of the Present Study

In the present study, the six-orientation single normal hot-wire technique is being employed to obtain the turbulence quantities in the combustor simulation confined jet flowfield. Measurements have been carried out for nonswirling flow with expansion angles of 90 degrees (sudden expansion) and 45 degrees (gradual expansion).

Chapter II gives background information on the various components of the experimental facility and the instruments employed for the hot-wire measurements.

The response equations using King's approach are given in Chapter III. Certain deviations from the procedures suggested by King are also included in this chapter. A thorough uncertainty analysis of the technique is carried out in order to judge the accuracy and the reliability of the six-orientation hot-wire technique. The salient features of the analysis are discussed in Chapter IV.

Turbulence quantities obtained, using this hot-wire technique, are part of Chapter V which discusses the results in detail. Some of the turbulence quantities are compared with measurements done by Chaturvedi (5) using cross-wire probe in a corresponding flow situation. Chapter VI concludes by summarizing the major achievements of the present study and suggesting some avenues for further research activity.

CHAPTER II

EXPERIMENTAL FACILITY AND INSTRUMENTATION

2.1 Idealized Flowfield

The facility, designed and built at Oklahoma State University, is a simulation of a typical axisymmetric combustion chamber of a gas turbine engine shown in Figure 1, Appendix B. The schematic of the test facility with idealized flowfield is shown in Figure 3, Appendix B. Ambient air enters the low-speed wind tunnel through a rubber foam air filter. Next the air flows through an axial flow fan driven by a 5 h.p. varidrive motor. Thus the flow rate can be varied for different test conditions. Then the flow is gradually expanded through the tunnel cross-section without separation because numerous fine mesh screens are encountered by the flow along the way.

Next, the flow goes through a turbulence management section which has two fine-mesh screens, a 12.7 cm length of packed straws, and five more fine-mesh screens. When the flow passes through the turbulence section, small eddies are formed which dissipate much quicker than the large eddies. The turbulence management section thus keeps the turbulence level down.

Having left the turbulence management section, the air enters into a contoured nozzle leading to the test section. This axisymmetric nozzle was designed to produce a minimum adverse pressure gradient on the boundry layer to avoid flow unsteadiness associated with local separation regions. The area ratio of the cross sections of the turbulence management section to that of the nozzle throat is approximately 22.5. The diameter, d, of the nozzle throat is approximately 15 cm.

Next, the air enters the test section. The test section is composed of a swirler (optional), an expansion block, and a long plexiglass tube. The swirler currently available is a variable vane-angle type device to impart swirl to the flow entering the test section. The expansion block, attached after the swirler, is a 30 cm diameter disk of wood. At present, there are three expansion blocks, and the appropriate choice gives α = 90, 70, or 45 degrees. The flow is expanded into a plexiglass tube of diameter, D, of 30 cm, thus giving diameter expansion ratio (D/d) of 2.

A typical real combustor, shown in Figure 1, Appendix B, is idealized in the present study, as there are no film cooling holes or dilution air holes, and the chamber wall of the test section is a constant diameter pipe. The test section is carefully aligned using a laser beam so that the test section and wind tunnel centerline are colinear.

2.2 Hot-Wire Instrumentation

Figure 4, Appendix B, shows the circuit diagram for a constant temperature anemometer. The anemometer used for the present study is DISA type 55M01, CTA standard bridge. A normal hot-wire, type 55P01, manufactured by DISA, is used to carry out the measurements of time-mean and root-mean-square voltages. These probes have two prongs set approximately 3 mm apart and carry 5 μm diameter wire which is gold plated near the prongs to reduce end effects and strengthen the wire. The time-mean voltage is measured with Hickok Digital Systems, Model DP100, integrating voltmeter and the root-mean-square voltage is measured using Hewlett Packard, Model 400 HR, voltmeter.

The hot-wire is mounted on the facility with the help of a traversing mechanism shown in Figure 5, Appendix B. It consists of a base that is modified to be mounted on the plexiglass tube of the text section at various axial locations. The hot-wire probe is inserted into the tube through a rotary vernier and the base. The rotary vernier is attached to a slide which can traverse up to approximately 14.5 cm. Thus it becomes possible for the probe to be traversed at any location in the combustor flowfield and rotated through 180 degrees. Figure 6, Appendix B, shows the test section with the probe mounted on it.

2.3 Calibration Nozzle

The hot-wire is calibrated on a small air jet. The facility consists of a compressed air line, which delivers the desired flow rate through a small pressure regulator and a Fischer and Porter Model 10A1735A rotameter. The jet housing consists of an effective flow management section followed by a contoured nozzle with a 3.5 cm diameter throat.

A rotary table is used to hold the probe while it is being calibrated in three different orientations which are discussed in Chapter III.

CHAPTER III

STATISTICAL ANALYSIS PROCEDURE

3.1 Response Equations

The six-orientation hot-wire technique requires a single, straight, hot-wire to be calibrated for three different probe directions in order to determine the directional sensitivity of such a probe. The three directions and the three calibration curves are shown in Figure 7, Appendix B. Each of the three calibration curves is obtained with zero velocity in the other two directions. The calibration curves demonstrate that the hot-wire is most efficiently cooled when the flow is in the $\hat{v}$ direction. Whereas, the wire is most inefficiently cooled for the flow in $\hat{w}$ direction. Each of the calibration curves follows a second order, least square fit, of the form:

$$E^2 = A + BZ^{\frac{1}{2}} + CZ \tag{1}$$

where A, B, and C are the calibration constants and Z can take a value of $\hat{u}$, $\hat{v}$, and $\hat{w}$ for the three calibration curves, respectively.

When the wire is placed in a 3-dimensional flowfield, the effective cooling velocity experienced by the hot-wire, in terms of the probe coordinator and pitch and yaw factors (G and K) as defined by Jorgensen (20) is:

$$Z^2 = \hat{v}^2 + G^2\hat{u}^2 + K^2\hat{w}^2 \tag{2a}$$

$$G = \frac{\hat{v}\ (\hat{w},\ \hat{u} = 0)}{\hat{u}\ (\hat{w},\ \hat{v} = 0)}\ , \tag{2b}$$

$$K = \frac{\hat{v}\ (\hat{w},\ \hat{u} = 0)}{\hat{w}\ (\hat{v},\ \hat{u} = 0)}\ , \tag{2c}$$

evaluated from the three calibration curves for a constant value of E^2.

To carry out measurements in the combustor flowfield, the wire is aligned in the flow in such a way that in the first orientation, the wire is normal to the flow in the axial direction and the probe coordinates coincide with the coordinates of the experimental facility. Thus the six equations for the instantaneous cooling velocities at the six orientations, as given by King (21) are:

$$Z_1^2 = v^2 + G^2u^2 + K^2w^2 \tag{3}$$
$$Z_2^2 = v^2 + G^2(u \cos 30^o + w \sin 30^o)^2 + K^2(w \cos 30^o - u \sin 30^o)^2 \tag{4}$$
$$Z_3^2 = v^2 + G^2(u \cos 60^o + w \sin 60^o)^2 + K^2(w \cos 60^o - u \sin 60^o)^2 \tag{5}$$
$$Z_4^2 = v^2 + G^2w^2 + K^2u^2 \tag{6}$$
$$Z_5^2 = v^2 + G^2(w \sin 120^o + u \cos 120^o)^2 + K^2(u \sin 120^o - w \cos 120^o)^2 \tag{7}$$
$$Z_6^2 = v^2 + G^2(w \sin 150^o + u \cos 150^o)^2 + K^2(u \sin 150^o - w \cos 150^o)^2 \tag{8}$$

Replacing the sines and cosines and expanding the square brackets:

$$Z_1^2 = v^2 + G^2u^2 + K^2w^2 \tag{3a}$$
$$Z_2^2 = v^2 + G^2(u^2\frac{3}{4} + \frac{w^2}{4} + uw\ \frac{\sqrt{3}}{2}) + K^2(w^2\frac{3}{4} + \frac{u^2}{4} - uw\ \frac{\sqrt{3}}{2}) \tag{4a}$$
$$Z_3^2 = v^2 + G^2(\frac{u^2}{4} + w^2\frac{3}{4} + uw\ \frac{\sqrt{3}}{2}) + K^2(\frac{w^2}{4} + u^2\frac{3}{4} - uw\ \frac{\sqrt{3}}{2}) \tag{5a}$$
$$Z_4^2 = v^2 + G^2w^2 + K^2u^2 \tag{6a}$$
$$Z_5^2 = v^2 + G^2(\frac{u^2}{4} + w^2\frac{3}{4} - uw\ \frac{\sqrt{3}}{2}) + K^2(\frac{w^2}{4} + u^2\frac{3}{4} + uw\ \frac{\sqrt{3}}{2}) \tag{7a}$$
$$Z_6^2 = v^2 + G^2(u^2\frac{3}{4} + \frac{w^2}{4} - uw\ \frac{\sqrt{3}}{2}) + K^2(w^2\frac{3}{4} + \frac{u^2}{4} + uw\ \frac{\sqrt{3}}{2}) \tag{8a}$$

Solving simultaneously any three adjacent equations provides expressions for the instantaneous values of the three velocity components, u, w, and v, in terms of the equivalent cooling velocities (Z_1, Z_2, and Z_3 for example, when the first three equations are chosen). King refers to these instantaneous velocity components as F1, F2, and F3 as follows:

$$F1 = \left[\left\{ AO + \left(AO^2 + \frac{BO^2}{3}\right)^{\frac{1}{2}} \right\} * \frac{1}{(G^2 - k^2)} \right]^{\frac{1}{2}} \tag{9}$$

$$F2 = \left[\left\{ -AO + \left(AO^2 + \frac{BO^2}{3}\right)^{\frac{1}{2}} \right\} * \frac{1}{(G^2 - K^2)} \right]^{\frac{1}{2}} \tag{10}$$

$$F3 = \left[CO - \frac{(G^2 + k^2)}{(G^2 - k^2)} * \left(AO^2 + \frac{BO^2}{3}\right)^{\frac{1}{2}} \right]^{\frac{1}{2}} \tag{11}$$

The values of AO, BO, and CO depend on the set of the three equations chosen and are given in Table 1, Appendix A, for appropriate equation sets.

However, these equations cannot be directly used because it is impossible to obtain Z_1, Z_2, and Z_3 at a single instance in time. There fore Equation 9 through 11 must be expressed in terms of mean and root-mean-square values. Equation 1 can be written as:

$$\phi(E_i) = Z_i = \left[\left[-B + \left\{ B^2 - 4C\,(A - E_i^2) \right\}^{\frac{1}{2}} \right] / 2c \right]^{\frac{1}{2}} \tag{12}$$

The above equation is in terms of instantaneous velocity Z_i and instantaneous voltage E_i. In order to obtain an expression for time-mean velocity as a function of time-mean voltage, a Taylor series expansion of Equation 12 can be carried out.

Since $Z_i = \phi(\overline{E}_i + E_i')$

$$Z_i = \phi(\overline{E}_i + E_i') = \phi(\overline{E}_i) + \frac{E_i'}{1!} \cdot \frac{\partial \phi}{\partial E_i} + \frac{{E_i'}^2}{2!} \cdot \frac{\partial^2 \phi}{\partial E_i^2} \tag{13}$$

The Taylor series is truncated after second order terms assuming the higher order terms to be relatively small. Time averaging both sides of the above equation and employing the fact that $\overline{E'} = 0$, yields:

$$\overline{Z}_i = \overline{\phi} + \tfrac{1}{2} \frac{\partial^2 \phi}{\partial E_i^2} \cdot \sigma_{E_i}^2 \tag{14}$$

where $\overline{\phi}$ indicates that the function is evaluated for $\overline{E}_i$. To obtain $\overline{Z_i'^2} = \sigma_{Z_i}^2$, the relationship as given by Hinze (13) is:

$$\overline{Z_i'^2} = \sigma_{Z_i}^2 = \text{Expec } [Z_i^2] - (\text{Expec } [Z_i])^2 \tag{15}$$

$$\text{Since Expec } [Z_i^2] \approx \overline{\phi} + 1/2 \frac{\partial^2 \phi}{\partial \overline{E}_i^2} \cdot \sigma_{E_i}^2, \tag{16}$$

the differential in Equation 16 can be evaluated as:

$$\frac{\partial^2 \overline{\phi^2}}{\partial E_i^2} = 2\left(\frac{\partial \overline{\phi}}{\partial E_i}\right)^2 + 2\overline{\phi} \cdot \frac{\partial^2 \overline{\phi}}{\partial E_i^2} \tag{17}$$

Then Equation 16 becomes:

$$\text{Expec } [Z_i^2] \simeq \overline{\phi}^2 + \left(\frac{\partial \overline{\phi}}{\partial E_i}\right)^2 \cdot \sigma_{E_i}^2 + \overline{\phi} \cdot \frac{\partial^2 \overline{\phi}}{\partial E_i^2} \cdot \sigma_{E_i}^2 \tag{18}$$

Squaring Equation 14 and substituting with Equation 18 into Equation 15 gives:

$$\overline{Z_i'^2} = \sigma_{Z_i}^2 \approx \frac{\partial \overline{\phi}}{\partial \overline{E}_i}^2 \cdot \sigma_{E_i}^2 - \left(1/2 \frac{\partial^2 \overline{\phi}}{\partial \overline{E}_i^2} \cdot \sigma_{E_i}^2\right)^2 \tag{19}$$

Thus Equations 14 and 19 give the mean and variance of individual cooling velocities in terms of the mean and variance of the appropriate voltage.

In a 3-dimensional flow, it is usually desired to obtain the mean and variance for the individual velocity components in axial, azimuthal, and radial directions, and also their cross correlations.

The procedure to obtain the mean and variance of the individual velocity components is the same as for the effective cooling velocities except that u, w, and v are functions of three random variables and there are extra terms in the Taylor expansion to account for the covariances of the cooling velocities. Thus the three mean volicities as given by Dvorak and Syred (19) and King (21) are:

$$\bar{u} = F1(Z_P, Z_Q, Z_R) + \frac{1}{2} \sum_{i=1}^{3} \frac{\partial^2 F1}{\partial Z_i^2} \cdot \sigma_{Z_i}{}^2 + \sum_{i<j}^{3} \frac{\partial^2 F1}{\partial Z_i \partial Z_j} \cdot K_{Z_i Z_j}, \tag{20}$$

where time-mean values are to be understood on the right side of this and subsequent equations.

$$\bar{w} = F2(Z_P, Z_Q, Z_R) + \frac{1}{2} \sum_{i=1}^{3} \frac{\partial^2 F2}{\partial Z_i^2} \cdot \sigma_{Z_i}{}^2 + \sum_{i<j}^{3} \frac{\partial^2 F2}{\partial Z_i \partial Z_j} \cdot K_{Z_i Z_j}, \tag{21}$$

and

$$\bar{v} = F3(Z_P, Z_Q, Z_R) + \frac{1}{2} \sum_{i=1}^{3} \frac{\partial^2 F3}{\partial Z_i^2} \cdot \sigma_{Z_i}{}^2 + \sum_{i<j}^{3} \frac{\partial^2 F3}{\partial Z_i \partial Z_j} \cdot K_{Z_i Z_j} \tag{22}$$

where $K_{Z_i Z_j}$ is the covariance of the cooling velocity fluctuations and is defined as:

$$K_{Z_i Z_j} = \frac{1}{T} \int_0^T (Z_i - \bar{Z}_i)(Z_j - \bar{Z}_j) dt \tag{23}$$

Also the normal stresses are given as:

$$\overline{u'^2} = \sum_{i=1}^{3} \left(\frac{\partial F1}{\partial Z_i}\right)^2 \cdot \sigma_{Z_i}{}^2 + \sum_{\substack{i \\ i \neq j}}^{3} \sum_{j}^{3} \frac{\partial F1}{\partial Z_i} \cdot \frac{\partial F1}{\partial Z_j} - \left[\frac{1}{2} \sum_{i=1}^{3} \frac{\partial^2 F1}{\partial Z_i^2} \cdot \sigma_{Z_i}{}^2 + \sum_{i<j}^{3} \frac{\partial^2 F1}{\partial Z_i \partial Z_j} \cdot K_{Z_i Z_j}\right]^2, \tag{24}$$

$$\overline{w'^2} = \sum_{i=1}^{3} \left(\frac{\partial F2}{\partial Z_i}\right)^2 \cdot \sigma_{Z_i}{}^2 + \sum_{\substack{i \\ i \neq j}}^{3} \sum_{j}^{3} \frac{\partial F2}{\partial Z_i} \cdot \frac{\partial F2}{\partial Z_j} - \left[\frac{1}{2} \sum_{i=1}^{3} \frac{\partial^2 F2}{\partial Z_i^2} \cdot \sigma_{Z_i}{}^2 + \sum_{i<j}^{3} \frac{\partial^2 F2}{\partial Z_i \partial Z_j} \cdot K_{Z_i Z_j}\right]^2, \tag{25}$$

and

$$\overline{v'^2} = \sum_{i=1}^{3} \left(\frac{\partial F3}{\partial Z_i}\right)^2 \cdot \sigma Z_i^{\,2} + \sum_{\substack{i \\ i \neq j}}^{3} \sum_{j}^{3} \frac{\partial F3}{\partial Z_i} \cdot \frac{\partial F3}{\partial Z_j} - \left[\frac{1}{2} \sum_{i=1}^{3} \frac{\partial^2 F3}{\partial Z_i^{\,2}} \cdot \sigma_{Z_i}^{\,2} + \right.$$

$$\left. \sum_{i<j}^{3} \frac{\partial^2 F3}{\partial Z_i \partial Z_j} \cdot K_{Z_i Z_j} \right]^2 , \qquad (26)$$

Also the shear stresses as given by Dvorak and Syred (19) are:

$$\overline{u'w'} = \sum_{i=1}^{3} \frac{\partial F1}{\partial Z_i} \cdot \frac{\partial F2}{\partial Z_i} \cdot \sigma_{Z_i}^{\,2} + \sum_{\substack{i \\ i \neq j}}^{3} \sum_{j}^{3} \frac{\partial F1}{\partial Z_i} \cdot \frac{\partial F2}{\partial Z_j} \cdot K_{Z_i Z_j} - \left[\frac{1}{2} \sum_{i=1}^{3} \frac{\partial^2 F1}{\partial Z_i^{\,2}} \cdot \sigma_{Z_i}^{\,2} \right.$$

$$\left. + \sum_{\substack{i \\ i<j}}^{3} \sum_{j}^{3} \frac{\partial^2 F1}{\partial Z_i \partial Z_j} \cdot K_{Z_i Z_j} \right] \left[\frac{1}{2} \sum_{i=1}^{3} \frac{\partial^2 F2}{\partial Z_i^{\,2}} \cdot \sigma_{Z_i}^{\,2} + \sum_{\substack{i \\ i<j}}^{3} \sum_{j}^{3} \frac{\partial^2 F2}{\partial Z_i \partial Z_j} \cdot K_{Z_i Z_j} \right] \qquad (27)$$

$$\overline{u'v'} = \sum_{i=1}^{3} \frac{\partial F1}{\partial Z_i} \cdot \frac{\partial F3}{\partial Z_i} \cdot \sigma_{Z_i}^{\,2} + \sum_{\substack{i \\ i \neq j}}^{3} \sum_{j}^{3} \frac{\partial F1}{\partial Z_i} \cdot \frac{\partial F3}{\partial Z_i} \cdot K_{Z_i Z_j} - \left[\frac{1}{2} \sum_{i=1}^{3} \frac{\partial^2 F1}{\partial Z_i^{\,2}} \cdot \sigma_{Z_i}^{\,2} \right.$$

$$\left. + \sum_{\substack{i \\ i<j}}^{3} \sum_{j}^{3} \frac{\partial^2 F1}{\partial Z_i \partial Z_j} \cdot K_{Z_i Z_j} \right] \left[\frac{1}{2} \sum_{i=1}^{3} \frac{\partial^2 F3}{\partial Z_i^{\,2}} \cdot \sigma_{Z_i}^{\,2} + \sum_{\substack{i \\ i<j}}^{3} \sum_{j}^{3} \frac{\partial^2 F3}{\partial Z_i \partial Z_j} \cdot K_{Z_i Z_j} \right] \qquad (28)$$

and finally,

$$\overline{w'v'} = \sum_{i=1}^{3} \frac{\partial F2}{\partial Z_i} \cdot \frac{\partial F3}{\partial Z_i} \cdot \sigma_{Z_i}^{\,2} + \sum_{\substack{i \\ i \neq j}}^{3} \sum_{j}^{3} \frac{\partial F2}{\partial Z_i} \cdot \frac{\partial F3}{\partial Z_j} \cdot K_{Z_i} - \left[\frac{1}{2} \sum_{i=1}^{3} \frac{\partial^2 F2}{\partial Z_i^{\,2}} \cdot \sigma_{Z_i}^{\,2} + \right.$$

$$\left. \sum_{\substack{i \\ i<j}}^{3} \sum_{j}^{3} \frac{\partial^2 F2}{\partial Z_i \partial Z_j} \cdot K_{Z_i Z_j} \right] \left[\frac{1}{2} \sum_{i=1}^{3} \frac{\partial^2 F3}{\partial Z_i^{\,2}} \cdot \sigma_{Z_i}^{\,2} + \sum_{\substack{i \\ i<j}}^{3} \sum_{j}^{3} \frac{\partial^2 F3}{\partial Z_i \partial Z_j} \cdot K_{Z_i Z_j} \right]$$

$$(29)$$

3.2 Calculation of Covariances

Dvorak and Syred (19) used a DISA time correlator (55A06) to find the correlation coefficients between the velocity fluctuations in the three directions. The method adopted by King (21) is to use the information obtained by all six orientations and devise a mathematical procedure to calculate the covariances.

The covariance matrix as derived by King is:

$$\left[K_{Z_i Z_j}\right] = \left[\Pi\right]\left[T\right]^{-1} \tag{30}$$

where

$$K_{Z_i Z_j} = \begin{bmatrix} K_{Z_P Z_Q} \\ K_{Z_P Z_R} \\ K_{Z_Q Z_R} \end{bmatrix},$$

and

$$\Pi = \begin{bmatrix} \Pi_1 \\ \Pi_2 \\ \Pi_3 \end{bmatrix}$$

where

$$\Pi_1 = \overline{Z}_{P+3} - \rho_1 - \frac{1}{2}\sum_{i=P}^{R} \frac{\partial^2 \rho_1}{\partial Z_i^{\,2}} \cdot \sigma_{Z_i}^{\;2}, \tag{31}$$

$$\Pi_2 = \overline{Z}_{P+4} - \rho_2 - \frac{1}{2}\sum_{i=P}^{R} \frac{\partial^2 \rho_2}{\partial Z_i^{\,2}} \cdot \sigma_{Z_i}^{\;2}, \tag{32}$$

and

$$\Pi_3 = \bar{Z}_{P+5} - \rho_3 - \frac{1}{2} \sum_{i=p}^{R} \frac{\partial^2 \rho_3}{2 Z_i{}^2} \cdot \sigma_{Z_i}{}^2 \tag{33}$$

Also

$$\rho_1 = \bar{Z}_P{}^2 - 2\bar{Z}_Q{}^2 + 2\bar{Z}_R{}^2 \tag{34}$$

$$\rho_2 = 2\bar{Z}_P{}^2 + 3\bar{Z}_Q{}^2 + 2\bar{Z}_R{}^2 \tag{35}$$

and $$\rho_3 = 2\bar{Z}_P{}^2 - 2\bar{Z}_Q{}^2 + \bar{Z}_R{}^2 \tag{36}$$

Matrix (T) is a three by three matrix and is given in Table II.

King discovered that matrix (T) is a singular matrix for all cases and hence equation 30 cannot be solved. Therefore, to get covariances one needs extra information. King has made an assumption about the relationship between the covariances in the form:

$$K_{Z_P Z_R} = \eta \frac{K_{Z_P Z_Q} \cdot K_{Z_Q Z_R}}{\sigma^2_{Z_Q}} \tag{37}$$

Where η is given a numerical value of 0.8.

Also $K_{Z_P Z_Q}$ is obtained from the quadratic equation:

$$K^2_{Z_P Z_Q} \left[\frac{-2\bar{Z}_P{}^2 \cdot \eta}{\sigma^2_{Z_Q}} \right] \mp K_{Z_P Z_Q} \left[6\bar{Z}_P \bar{Z}_Q - \frac{\bar{Z}_P}{\bar{Z}_Q \sigma_{Z_Q}{}^2} (\Pi 1 \cdot \bar{Z}^3_{R+1} - \Pi 3 \cdot \bar{Z}^3_{R+3}) \right] + \left[\Pi 1 \cdot \bar{Z}^3_{R+1} - 2\Pi 3 \cdot \bar{Z}^3_{R+3} \right] = 0 \tag{38}$$

Equation 38 provides the two values for $K_{z_P z_Q}$. The covariance is related to the correlation coefficient as:

$$\gamma_{Z_P Z_Q} = \frac{K_{Z_P Z_Q}}{[\sigma_{Z_P}{}^2 \cdot \sigma_{Z_Q}{}^2]^{\frac{1}{2}}} \tag{39}$$

where $-1 < \gamma_{z_i z_j} < 1$

Therefore, Equation 39 is written in the form:

$$K_{Z_P Z_Q} = \gamma_{Z_P Z_Q} \cdot \left[\sigma_{Z_P}{}^2 \cdot \sigma_{Z_Q}{}^2\right]^{\frac{1}{2}} \tag{40}$$

The two calculated values of $K_{z_P z_Q}$ from equation 38 are then substituted in Equation 39, and the two corresponding values of $\gamma_{z_P z_Q}$ are calculated. The correlation coefficient which lies within the required range of $\pm$ 1, is used. For the case when the absolute values of both the correlation coefficients are larger than 1, the covariance is given by

$$K_{Z_P Z_Q} = 0.9 \left[\sigma_{z_p}^2 \cdot \sigma_{z_Q}^2\right]^{\frac{1}{2}} \tag{41}$$

Having calculated $K_{z_P z_Q}$, $K_{z_Q z_R}$ can be calculated from the relationship:

$$K_{Z_Q Z_R} = \frac{1}{2.\bar{Z}_Q \bar{Z}_R} \left[2.\bar{Z}_P . \bar{Z}_Q . K_{Z_P Z_Q} + \Pi_1 . \bar{Z}^3_{P+3} - \Pi_3 . \bar{Z}^3_{P+5}\right] \tag{42}$$

A similar test is applied to ensure that the absolute value of $\gamma_{z_Q z_R}$ is less than one otherwise $K_{z_Q z_R}$ is calculated from the relationship:

$$K_{Z_Q Z_R} = 0.9 \left[\sigma_Q{}^2 . \ \sigma_R{}^2\right]^{\frac{1}{2}} \tag{43}$$

$K_{z_p z_R}$ can now be calculated from equation 37. The calculated value of $K_{z_p z_Q}$, $K_{z_Q z_R}$, and $K_{z_p z_R}$ can now be substituted in equations 20 thru 22, and 24 thru 29 to calculate the mean velocities and Reynold stresses.

It was observed during the present study that King's method is not self-consistent in calculating the covariances. The correlation coefficients were found to have values greater than one and therefore it was necessary to have a more consistent method to calculate the covariances. Occasionally, King's method assumed that $\gamma_{z_p z_Q}$ and $\gamma_{z_Q z_R}$ had values of 0.9 and $\gamma_{z_p z_R}$ had a value of 0.648. But this was done only when some of the correlation coefficients were greater than one. The present method assumes constant values of the correlation coefficients. King has suggested that if two wires are separated by an angle of 30 degrees, the fluctuating signals from the wires at the two locations would be such that their contribution to the cooling of the wire would be related by the cosine of the angle between the wires therefore, $\gamma_{z_p z_Q}$ = cos 30° = 0.9 and similarly we would get

$$\gamma_{z_Q z_R} = 0.9,$$

also $\gamma_{z_p z_R} = \eta * \gamma_{z_p z_Q} * \gamma_{z_Q z_R} = 0.648$

Therefore the present method allows the covariances to be calculated using the following three equations:

$$K_{z_p z_Q} = 0.9 \left[\sigma_{z_p}^2 \cdot \sigma_{z_Q}^2\right]^{\frac{1}{2}} \tag{41}$$

$$K_{z_Q z_R} = 0.9 \left[\sigma_{z_Q}^2 \cdot \sigma_{z_R}^2\right]^{\frac{1}{2}} \tag{35}$$

$$K_{z_p z_R} = 0.648 \left[\sigma_{z_p}^2 \cdot \sigma_{z_R}^2\right]^{\frac{1}{2}} \tag{44}$$

CHAPTER IV

UNCERTAINTY ANALYSIS

An uncertainty analysis is presented here with a view to demonstrate the reliability of the six-orientation hot-wire technique and its sensitivity to various input parameters which have major contributions in the response equations. The analysis is done for both laminar and turbulent flow cases. The salient results are tabulated in Tables III and IV of Appendix A.

4.1 Effect of Pitch and Yaw Factors

Pitch and yaw factors (G and K) are used in the response equations described in Chapter III in order to compensate and account for the directional sensitivity of the single hot-wire probe. Figure 8, Appendix B, shows the pitch and yaw factors plotted against the hot-wire mean effective voltage. Both the pitch and yaw factors are functions of the hot-wire mean effective voltage, but the yaw factor is far more sensitive. A 10 percent increase in the voltage reduces the yaw factor by 56 percent and the pitch factor by 13 percent. The value of the pitch factor stays very close to one and hence does not have a major contribution in the response equations. For this reason, it is necessary to further consider the yaw factor, which is now examined for both laminar and turbulent flow conditions.

4.1.1 Laminar Flow

For laminar flow cases, the covariances $K_{z_i z_j}$ become zero and drop out of the response equations. Then Equations 20, 21, and 22 can be written as:

$$\bar{u} = F1\ (\bar{Z}_p, \bar{Z}_Q, \bar{Z}_R)$$
$$\bar{w} = F2\ (\bar{Z}_p, \bar{Z}_Q, \bar{Z}_R)$$
$$\bar{v} = F3\ (\bar{Z}_p, \bar{Z}_Q, \bar{Z}_R)$$

Experiments were performed on a calibration nozzle free jet in the potential core where the flow can be idealized as being laminar.

As Table III, Appendix A, shows, the effect of yaw factor on time-mean axial and swirl velocities is insignificant for the laminar flow case.

4.1.2 Turbulent Flow

The variation of yaw factor is studied on the turbulence quantities such as mean velocities, turbulence intensities and the shear stress $\overline{u'v'}$. As stated in Table III, all turbulence quantities behave differently to the variations in the yaw factor. The effect on all the turbulence quantities, except the mean radial velocity, is insignificant. In the case of mean radial velocity, the term (G^2-K^2) in the denominator of Equation 9 changes the value of F3 considerably for small changes in the yaw factor.

4.2 Effect of Correlation Coefficients

Correlation coefficients are used in Equation 40 to calculate the covariances between the fluctuations of the cooling velocities experienced by the hot-wire at adjacent orientations. These are then used in Equations 20 through 29 to calculate various turbulence quantities. A wide range of correlation coefficients ($\gamma_{z_P z_Q}$) between 0.1 to 0.9 are used to study the behavior of the turbulence quantities. Among all the turbulence quantities, $\overline{u'v'}$ was found to be most sensitive to variations in the correlation coefficient ($\gamma_{z_P z_Q}$). In view of the sensitivity of $\overline{u'v'}$ to $\gamma_{z_P z_Q}$ and the assumptions required to estimate $\gamma_{z_P z_Q}$, it is apparent that this is the major source of the significantly large uncertainty in the estimate of the turbulent shear stress. This appears to be an inherent deficiency of the six-orientation single hot-wire method.

King (21) used a parameter Eta (η) to relate the covariances between the fluctuations of the effective cooling velocities that are separated by 30 degrees with the covariance of velocities separated by 60 degrees (see Equation 37). He suggested a numerical value of 0.8 for η. Table III shows the effect of η on the turbulence quantities to be insignificant and hence the present study retains this value of 0.8 in all subsequent deductions.

4.3 Experimental Uncertainty

Experimental uncertainty was tested for both laminar and turbulent flow cases. The main reason for these tests was to determine the mean and variance of the output quantities when obtained from the six possible choices of three from among the six possible response equations (Equations 3 through 8 in Chapter III). Another objective of the study was to judge the extent of errors in output quantities because of errors in measurement of mean and root-mean-square voltages.

4.3.1 Laminar Flow

The calibration free jet facility was used to conduct laminar flow uncertainty experiments. To generate velocities in the axial and azimuthal direction with respect to the wire, the wire was offset by 45 degrees to the main direction of the flow and placed in the potential core region, thereby achieving two equal components of axial and swirl velocities. However, upon data reduction, it was observed that the two components were not equal. The variation among the two components was different for each choice of the six combinations of three adjacent response equations. In general, the variation among the two components was negligible.

Table III shows the effect of variations in measurements of the hot-wire mean voltages on the turbulence quantities. For laminar flow case, the mean axial and swirl velocities are extremely sensitive to errors in measurements of hot-wire mean voltage. This particular test stresses the need for using precise voltmeters. A 10 percent error in measurement of one of the six mean voltages leads to an error of 90 percent in axial velocity deduction for the conditions of this test. At other flow conditions, similar gross sensitivity may be expected.

Turbulence quantities are calculated using six different combinations of the three mean effective cooling velocities experienced by the hot-wire at three adjacent orientations. Table IV, Appendix A, demonstrates good consistency between the six possibilities for mean axial and swirl velocity determination in laminar flow conditions.

4.3.2 Turbulent Flow

As observed for the laminar flow case, errors in mean voltage measurements are extremely magnified in calculations of turbulence quantities. Table III shows these large variations in the turbulence quantities.

For turbulent flows, a large scatter is observed among the six values of turbulence quantities deduced from the six different combinations. To get an estimate of the scatter, the flowfield location x/D = 2.0, r/D = 0.25 for the case of side-wall angle α = 45 degrees was selected inside the main test facility. At this location in the flowfield, the turbulence quantities obtained are good representatives of turbulence level in the combustor flowfield.

Table IV shows that for turbulent flow, all the six combinations do not reveal all the turbulence quantities. The omitted items correspond to occasions when the velocity function F3 attains a complex value via the requirement of the square root of a negative value. Then, no further progress could be made with that particular set of three adjacent orientations in such situations.

Table IV also highlights the scatter among the six values of each turbulent quantity when solved using six different combinations. It is evident that certain quantities (such as mean radial velocity, the radial turbulence intensity, and the shear stress $\overline{u'v'}$) have very large scatter. This shows a great uncertainty in the use of six-orientation hot-wire technique in measurement of these quantities.

CHAPTER V

RESULTS

The six-orientation hot-wire technique is employed to measure the turbulence quantities for nonswirling conditions. The experiments have been conducted for expansion angles of 90 degrees (sudden expansion) and 45 degrees (gradual expansion). A computer program, listed in Appendix D, written in Fortran language, is used to process the data on an IBM 370/168 computer. For each location in the flowfield, six combinations of three adjacent orientations are selected and six values of each of the nine turbulence quantities are obtained. So, a decision has to be made about the selection of one of the six values. In nonswirling conditions, the flow is mainly dominated by the axial velocity. When the hot-wire is parallel to the axial direction; it experiences the least cooling effect from the axial velocity, whereas the radial and swirl velocities affect the wire most efficiently. Therefore, a small change in the v and w velocities will show a significant change in hot-wire voltage. Hence the set of orientations labeled (3, 4, 5) in Chapter III (orientation 4 having the hot-wire parallel to the x-direction) is chosen and used in all subsequent results presented, except where noted otherwise. Nevertheless, there are some quantities, such as v'_{rms} and $\overline{u'v'}$, which appear to be better represented by alternative sets of three adjacent orientations, but the appropriate choice is not known a priori.

5.1 Mean Velocities

Radial distributions of time-mean axial and radial velocities are plotted in Figures 9 and 10, Appendix B, respectively. Mean axial velocities for different axial locations and expansion angles are compared with measurements done with a crossed hot-wire probe by Chaturvedi (5). A good agreement is found between the two studies.

Because of the inability of the hot-wire to determine the sense of the flow direction, the presence of the corner recirculation zone was observed by a sudden increase in the axial velocity closer to the wall. Mean radial velocity was found to increase at the centerline with an increase in the axial distance. The mean velocity profiles tend to get flatter further downstream from the inlet. For $\alpha = 45°$, mean radial velocity at the centerline increased from 5 percent of the maximum inlet mean velocity at $x/D = 0.5$ to 16 percent of the maximum inlet velocity at $x/D = 2.0$. A similar increase was observed for $\alpha = 90°$.

5.2 Turbulence Intensities

The six-orientation hot-wire technique enables one to measure the axial, radial, and azimuthal turbulence intensities at various axial and radial locations in the confined jet flowfield. The radial distributions of these turbulence intensities are plotted in Figures 11, 12, and 13 of Appendix B. The axial and radial turbulence intensities are compared with Chaturvedi's study (5) and reasonable agreement is found in the case of axial turbulence intensities. However, the two studies are not in good agreement for radial turbulence intensities. The peak values measured in the present study are much lower, in certain cases being only 50 percent of the previously measured peak values (5). While solving the six sets of combinations of three adjacent orientations, it was found that $v'_{rms}/\bar{u}_0$ has a large scatter. For example at x/D = 2.0, r/D = 0.300, and α = 45°, the mean and the standard deviation of $v'_{rms}/\bar{u}_0$, among the six sets of readings, were found to be 0.1447 and 0.0330, respectively. This large scatter shows that in nonswirling flow this technique is not a very accurate way of measuring the radial turbulence intensities. Nevertheless, results shown in Figure 11 have been obtained with the set of orientations (3, 4, 5) being used.

5.3 Shear Stresses

In nonswirling flow conditions, measurements have been made of the turbulent shear stress $\overline{u'v'}$. The radial distribution of $\overline{u'v'}/u_0^2$ at various axial locations is plotted in Figure 14, Appendix B, and is compared with the earlier study done by Chaturvedi (5). In general, the two studies are in good agreement, but they do differ in two respects: the centerline values far downstream and the peak values near the inlet.

Chaturvedi (5) measured $\overline{u'v'}$ to be zero at the centerline at all axial locations. However, in the present study, $\overline{u'v'}$ is found to be nonzero at the centerline at axial locations greater than x/D = 0.5 for both side-wall angles α = 45° and α = 90°. A detailed study shows that the scatter for $\overline{u'v'}/u_0^2$, when calculated from different sets of adjacent orientations, is quite large. The ratio of standard deviation to the mean is approximately 0.6 and varies with position.

Peak values of $\overline{u'v'}$ are seen to be in good agreement except close to the inlet. At x/D = 0.5, Chaturvedi (5) measured peak values approximately 50 percent higher than in the present study. It must be remembered that there is always difficulty in measuring shear stress values in thin shear layer regions. In the present study, there is also the previously-discussed deficiency, see Chapter IV, because of the assumpitions made about the correlation coefficients $\gamma_{z_i z_j}$. These assumptions may be the major source of significantly large uncertainty in the calculation of turbulent shear stress values.

CHAPTER VI

CLOSURE

6.1 Summary

The six-orientation hot-wire technique is a relatively new method to measure time-mean values and turbulence quantities in complex three-dimensional flowfields. Applied in this study to nonreacting nonswirling axisymmetric flowfields, measurements of time-mean and root-mean-square voltages at six different orientations contain enough information to obtain the time-mean velocities, turbulence intensities and shear stresses. At each location in the flow, there are six different values of each of the above quantities that can be obtained by using six sets of measurements of three adjacent orientations. Because of axial velocity domination, a particular set of orientations was chosen. Nevertheless, the measurement accuracy can be well judged by the scatter of the values of turbulence quantities among the six different combinations of sets of three mean effective cooling velocities. The nonswirling confined jet flow was investigated with this technique. It was found to be an excellent method to find time-mean velocities. It also gave good results for turbulence intensities and shear stresses. An uncertainty analysis done on this technique reveals that certain output parameters such as the axial, radial, and azimuthal turbulence intensities and shear stresses are extremely sensitive to some input parameters such as yaw factor and mean voltages.

6.2 Further Work

The multi-orientation single-wire technique is a useful cost-effective tool for the investigation of complex flowfields. At present, there is a need to check repeatability under nonswirling conditions before progressing to the investigation of flows with moderate and strong swirl. This would lead to further evaluation of reliability and accuracy of the technique in general flowfields. Thus far, there is an *a priori* assumption about the evaluation of covariances, which entails the use of constant values for the correlation coefficients. Further work might call for the development of alternative methods to specify the covariances. Nevertheless, the method has potential for further use in the experimental evaluation of complex flowfields.

REFERENCES

(1) Lefebvre, A. H. (ed.). Gas Turbine Combustor Design Problems. New York: Hemisphere-McGraw-Hill, 1980.

(2) Rhode, D. L., "Predictions and Measurements of Isothermal Flowfields in Axisymmetric Combustor Geometries," Ph.D. Thesis, Oklahoma State University, Stillwater, Oklahoma, 1981.

(3) Rhode, D. L., D. G. Lilley, and D. K. McLaughlin. "On the Prediction of Swirling Flowfields Found in Axisymmetric Combustor Geometries." Proceedings, ASME Symposium on Fluid Mechanics of Combustion Systems. Boulder, Colo., June 22-24, 1981, pp. 257-266.

(4) Krall, K. M., and E. M. Sparrow. "Turbulent Heat Transfer in the Separated, Reattached, and Redevelopment Regions of a Circular Tube." Journal of Heat Transfer (Feb., 1966), pp. 131-136.

(5) Chaturvedi, M. C. "Flow Characteristics of Axisymmetric Expansions." Proceedings, Journal of the Hydraulics Division, ASCE, Vol. 89, No. HY3 (1963), pp. 61-92.

(6) Phaneuf, J. T., and D. W. Netzer. Flow Characteristics in Solid Fuel Ramjets. Report No. NPS-57Nt74081. Prepared for the Naval Weapons Center by the Naval Postgraduate School, Monterey, California, July, 1974.

(7) Back, L. H., and E. J. Roschke. "Shear Layer Flow Regimes and Wave Instabilities and Reattachment Lengths Downstream of an Abrupt Circular Channel Expansion." Journal of Applied Mechanics (Sept., 1972), pp. 677-681.

(8) Roschke, E. J., and L. H. Back. "The Influence of Upstream Conditions on Flow Reattachment Lengths Downstream of an Abrupt Circular Channel Expansion." Journal of Biomechanics, Vol. 9 (1976), pp. 481-483.

(9) Ha Minh, H., and P. Chassaing. "Pertubations of Turbulent Pipe Flow." Proceedings, Symposium on Turbulent Shear Flows. Pennsylvania State University, April, 1977, pp. 13.9-13.17.

(10) Moon, L. F., and G. Rudinger. "Velocity Distribution in an Abruptly Expanding Circular Duct." Journal of Fluids Engineering (March, 1977), pp. 226-230.

(11) Johnson, B. V., and J. C. Bennett. "Velocity and Concentration Characteristics and Their Cross Correlation for Coxial Jets in a Confined Sudden Expansion; Part II: Predictions." Proceedings, ASME Symposium on Fluid Mechanics of Combustion Systems. Boulder, Colo., June 22-23, 1981, pp. 145-160.

(12) Goldstein, S. (ed.). "Modern Developments in Fluid Dynamics," Vol. I and II. New York: Dover Publications, 1965.

(13) Hinze, J. O. "Turbulence," 2nd Edition. New York: McGraw-Hill, 1975.

(14) Bradshaw, P. An "Introduction to Turbulence and Its Measurement." New York: Pegamon Press, 1971.

(15) Beer, J. M., and N. A. Chigier. "Combustion Aerodynamics," New York, Halsted Press Division, John Wiley & Sons, Inc., 1972.

(16) Syred, N., J. M. Beer, and N. A. Chigier. "Turbulence Measurements in Swirling Recirculating Flows." Proceedings, Salford Symposium on Internal Flows. London, England: Inst. of Mechanical Engineering, 1971, pp. B27-B36.

(17) Wygnanski, I., and H. Fielder. "Some Measurements in the Self Preserving Jet." Journal of Fluid Mechanics, Vol. 38, 1969, p. 577.

(18) Pratte, B. D., and J. R. Keffer. "The Swirling Turbulent Jet." Journal of Basic Engineering, Vol. 94 (Dec., 1972), pp. 739-748.

(19) Dvorak, K., and N. Syred, "The Statistical Analysis of Hot Wire Anemometer Signals in Complex Flow Fields," DISA Conference, Univ. of Leicester, 1972.

(20) Jorgensen, F. E. "Directional Sensitivity of Wire and Fiber Film Probes." DISA Information No. 11, Franklin Lakes, NJ, May 1971.

(21) King, C. F. "Some Studies of Vortex Divices - Vortex Amplifier Performance Behavior," Ph.D. Thesis, Univ. College of Wales, Cardiff, Wales, 1978.

(22) Habib, M. A., and J. H. Whitelaw. "Velocity Characteristics of Confined Coaxial Jets With and Without Swirl." ASME Paper 79-WA/FE-21. New York, NY, Dec. 2-7, 1979.

(23) Gupta, A. K., and D. G. Lilley. Flowfield Modeling and Diagnostics. Tunbridge Wells, England: Abacus Press, 1982 (in press).

APPENDICES

APPENDIX A

TABLES

TABLE I

VALUES OF AO, BO, AND CO IN VARIOUS EQUATION SETS

Equation Set P,Q,R Choice	AO	BO	CO
1, 2, 3	$(Z_2^2 - Z_3^2)$	$(-2Z_1^2 + 3Z_2^2 - Z_3^2)$	$(Z_1^2 - Z_2^2 + Z_3^2)$
2, 3, 4	$(Z_2^2 - Z_3^2)$	$(-Z_2^2 + 3Z_3^2 - 2Z_4^2)$	$(Z_2^2 - Z_3^2 + Z_4^2)$
3, 4, 5	$(Z_3^2 - 2Z_4^2 + Z_5^2)$	$(Z_3^2 - Z_5^2)$	$(Z_3^2 - Z_4^2 + Z_5^2)$
4, 5, 6	$(-Z_5^2 + Z_6^2)$	$(-2Z_4^2 + 3Z_5^2 - Z_6^2)$	$(Z_4^2 - Z_5^2 + Z_6^2)$
5, 6, 1	$(-Z_5^2 + Z_6^2)$	$(-Z_5^2 + 3Z_6^2 - 2Z_1^2)$	$(Z_5^2 - Z_6^2 + Z_1^2)$
6, 1, 2	$(-Z_6^2 + 2Z_1^2 - Z_2^2)$	$(-Z_6^2 + Z_2^2)$	$(Z_5^2 - Z_1^2 + Z_2^2)$

TABLE II

Matrix (T) in Equation 30

$\frac{2\ Z_P\ Z_Q}{Z^3_{P+3}}$	$\frac{-2\ Z_P\ Z_R}{Z^3_{P+3}}$	$\frac{4\ Z_Q\ Z_R}{Z^3_{P+3}}$
$\frac{6\ Z_P\ Z_Q}{Z^3_{P+4}}$	$\frac{-4\ Z_P\ Z_R}{Z^3_{P+4}}$	$\frac{2\ Z_Q\ Z_R}{Z^3_{P+4}}$
$\frac{4\ Z_P\ Z_Q}{Z^3_{P+5}}$	$\frac{-2\ Z_P\ Z_R}{Z^3_{P+5}}$	$\frac{2\ Z_Q\ Z_R}{Z^3_{P+5}}$

TABLE III

EFFECT OF INPUT PARAMETERS ON TURBULENCE QUANTITIES

PARAMETER	TYPE OF FLOW	% CHANGE IN PARAMETER	% CHANGES IN TURBULENCE QUANTITIES						
			$\overline{u}$	$\overline{w}$	$\overline{v}$	u'_{rms}	w'_{rms}	v'_{rms}	$\overline{u'v'}$
K	LAM	+10	+0.14	+0.146	--	--	--	--	--
K	TURB	+10	-0.17	--	-5.96	-0.18	-0.18	+0.53	No Change
${}^{\gamma}Z_PZ_Q$	TURB	+10	+0.22	--	+2.76	-3.17	-8.15	-0.57	40.28
$\overline{E}_1$	LAM	+10	+89.2	+74.5	--	--	--	--	--
ALL $\overline{E}_i$ i=1,6	LAM	+10	+65.9	+65.4	--	--	--	--	--
η	TURB	+10	-0.50	--	+1.37	+4.64	+7.02	+0.88	-1.34
$\overline{E}_1$	TURB	+10	16.3	--	--	-32.8	--	--	+528.3
ALL $\overline{E}_i$ i=1,6	TURB	+10	+72.9	--	+97.2	+54.2	+61.7	+64.8	+118.8

TABLE IV

SCATTER AMONG THE TURBULENCE QUANTITIES WHEN SOLVED BY SIX DIFFERENT COMBINATIONS

TURBULENCE QUANTITY	TYPE OF FLOW	TURBULENCE QUANTITY SOLVED BY SIX COMBINATIONS						MEAN	STANDARD DEVIATION	PERCENT
		1,2,3	2,3,4	3,4,5	4,5,6	5,6,1	6,1,2	$\overline{x}$	σ	$\sigma/\overline{x}$
$\overline{u}$(m/s)	LAM	6.92	6.8566	7.1162	7.0224	6.7273	6.9326	6.9291	0.134	1.9
$\overline{w}$(m/s)	LAM	7.546	7.4879	7.4093	7.8195	7.557	7.4899	7.5513	0.1414	1.9
$\overline{u}/\overline{u}_o$	TURB	0.3478	0.3115	0.3343	0.3035	0.3398	0.2382	0.3125	0.0402	12.9
$\overline{v}/\overline{u}_o$	TURB	--	0.1818	0.1717	0.1795	0.560	0.1835	0.1545	0.0552	35.7
$u'_{rms}/\overline{u}_o$	TURB	0.1758	0.1781	0.1331	0.1711	0.1680	0.2511	0.1795	0.0387	21.6
$v'_{rms}/\overline{u}_o$	TURB	--	0.0778	0.0743	0.0783	0.0355	--	0.0665	0.0207	31.1
$\left[\overline{u'v'}/\overline{u}_o^{\,2}\right]^{1/2}$	TURB	--	0.136	0.059	0.100	0.0943	--	0.0973	0.0315	32.4
$\overline{u'v'}/\overline{u}_o^{\,2}$	TURB	0.0185	0.0035	0.0101	0.0036	--	--	0.0089	0.0071	79.8

APPENDIX B

FIGURES

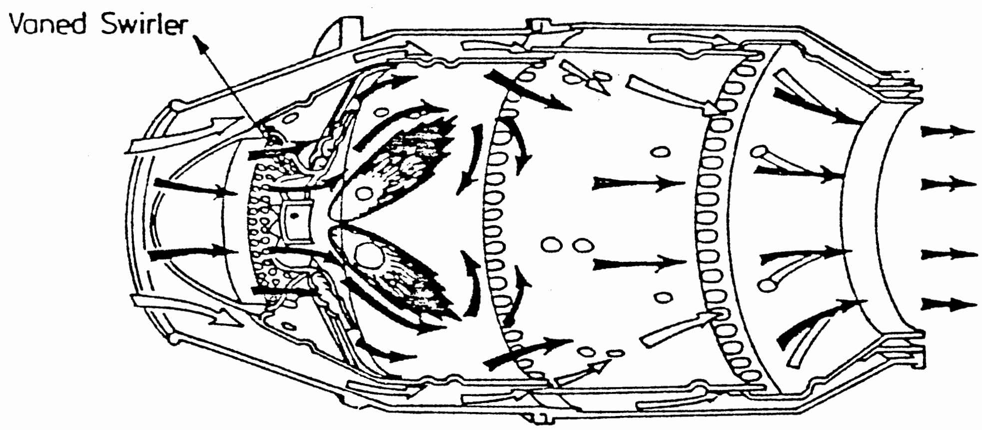

Figure 1. Typical Axisymmetric Combustion Chamber of a Gas Turbine Engine

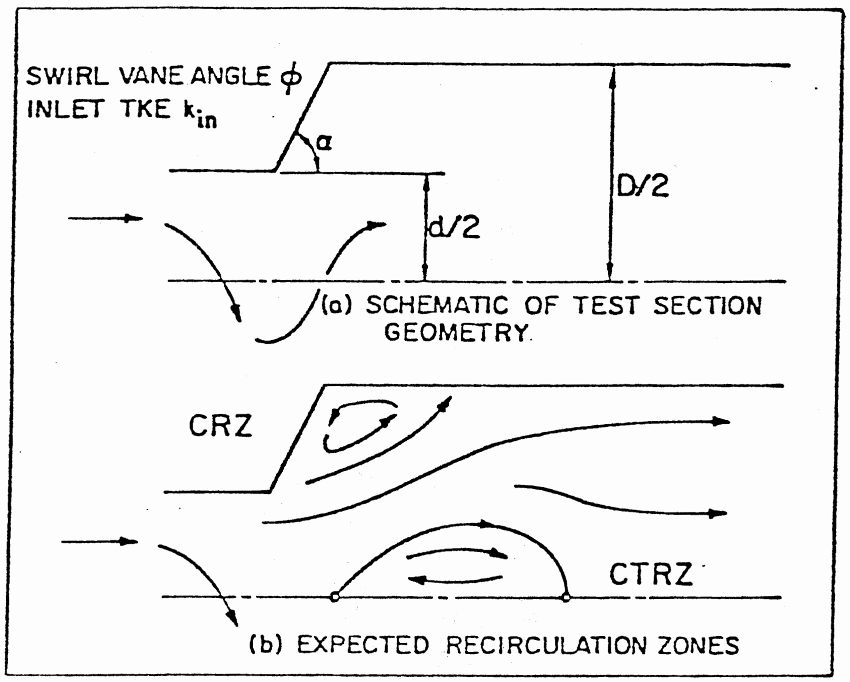

Figure 2. The Flowfield Being Investigated

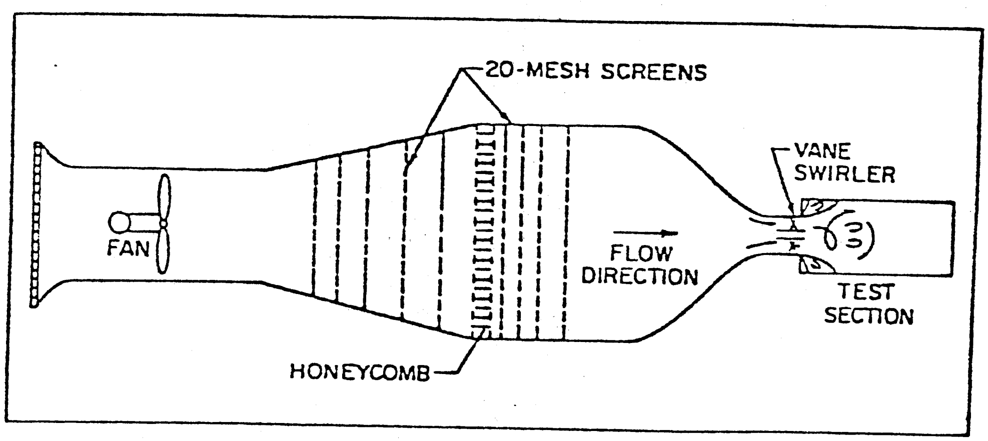

Figure 3. Schematic of Overall Facility

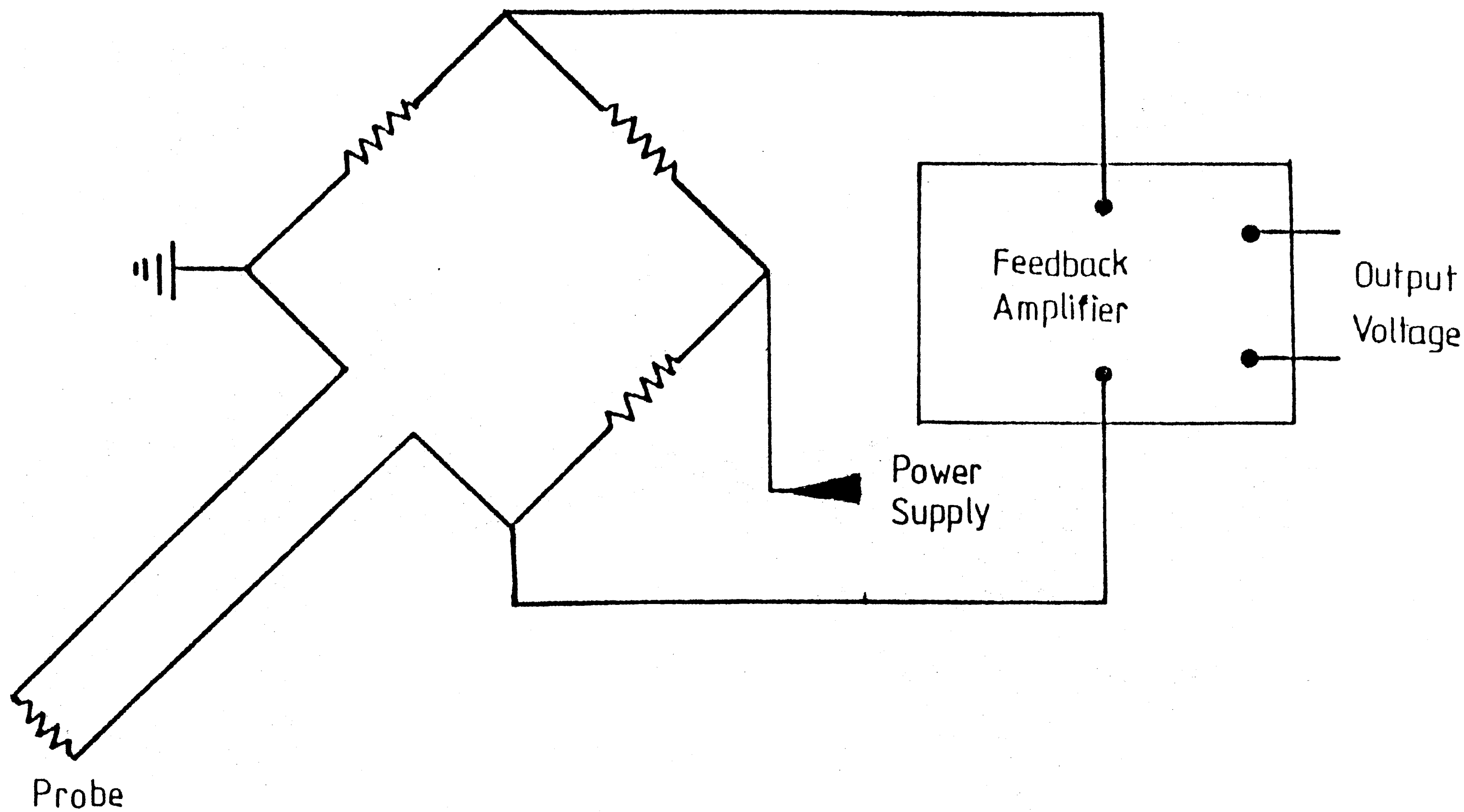

Figure 4. Hot-Wire Constant Temperature Anemometer

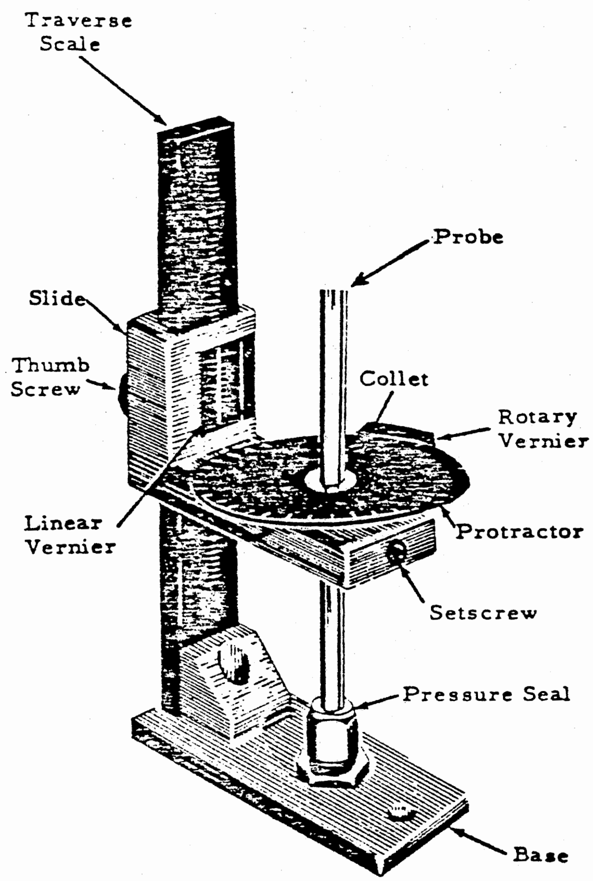

Figure 5. Manual Traversing Mechanism Used for Hot-Wire Orientations in the Flowfield

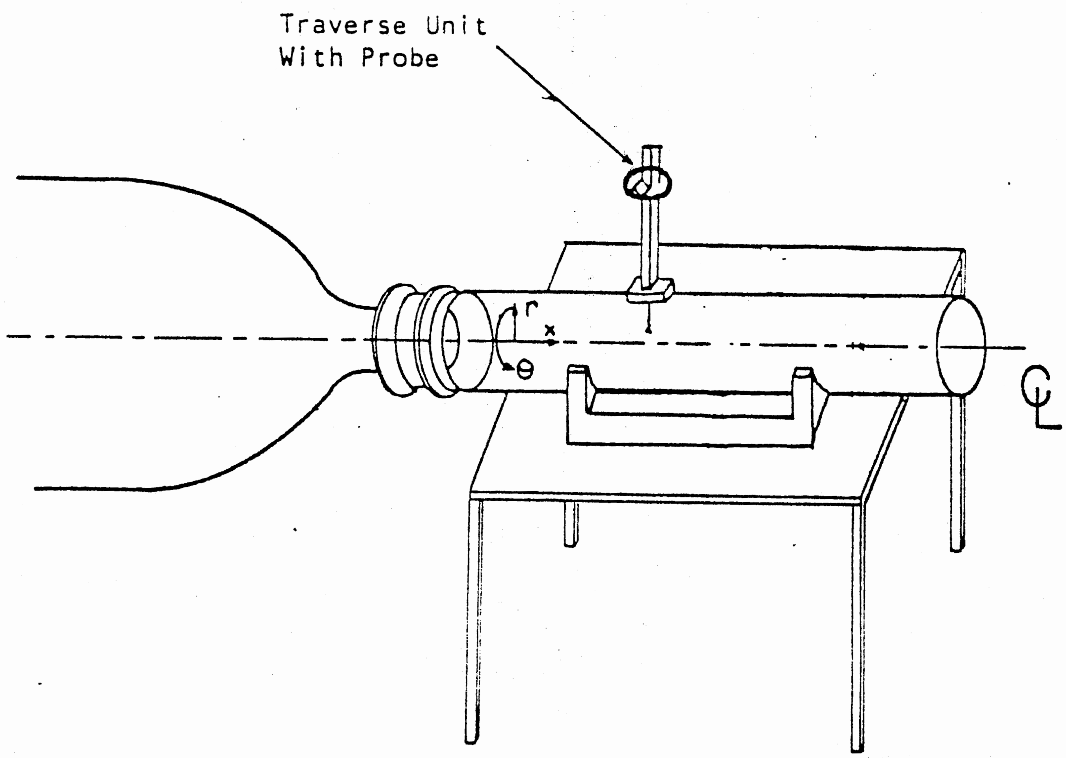

Figure 6. Mounting the Hot-Wire Probe on the Test Section

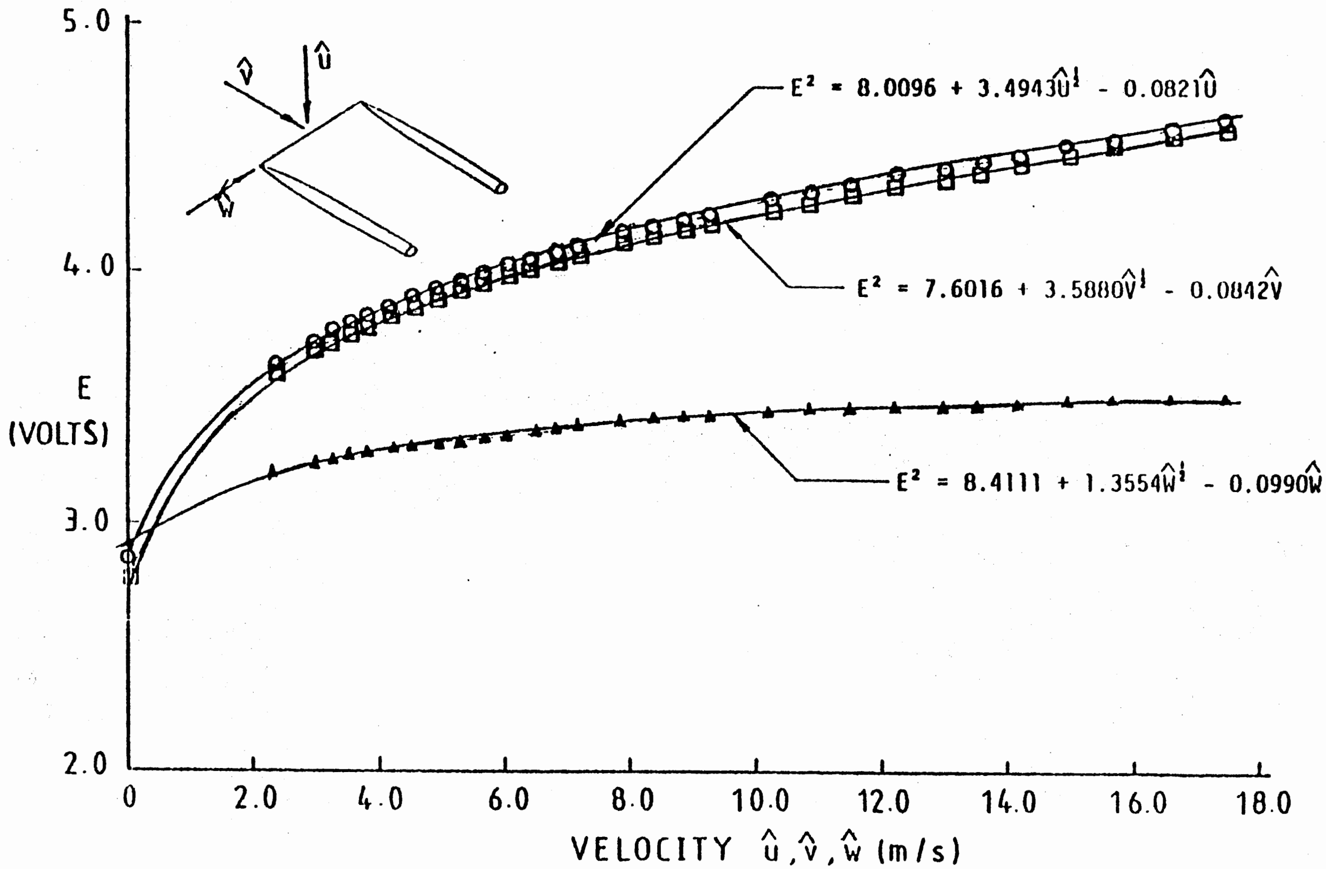

Figure 7. The Three-Directional Hot-Wire Calibration

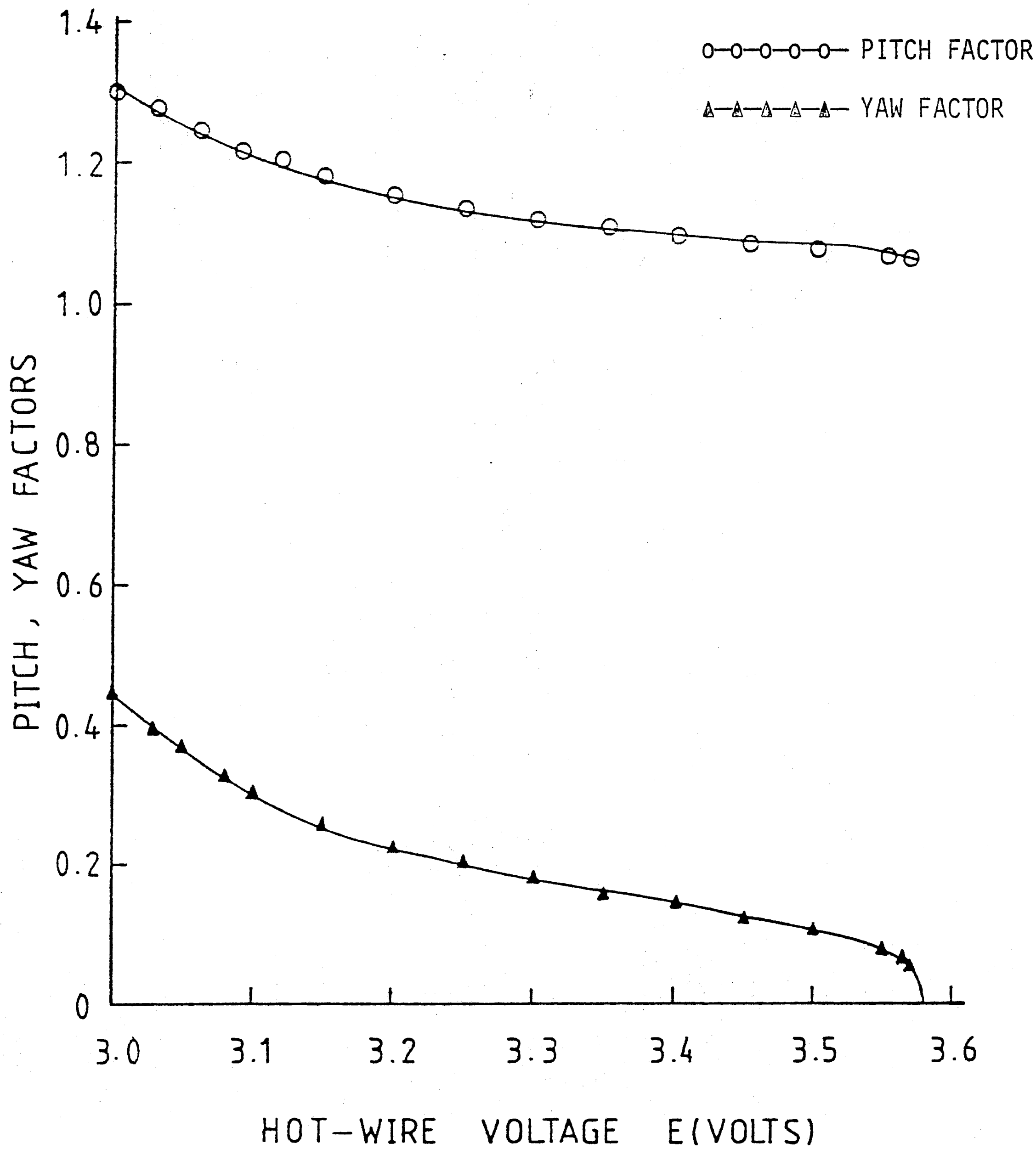

Figure 8. Plot of Pitch and Yaw Factors Versus Hot-Wire Voltage

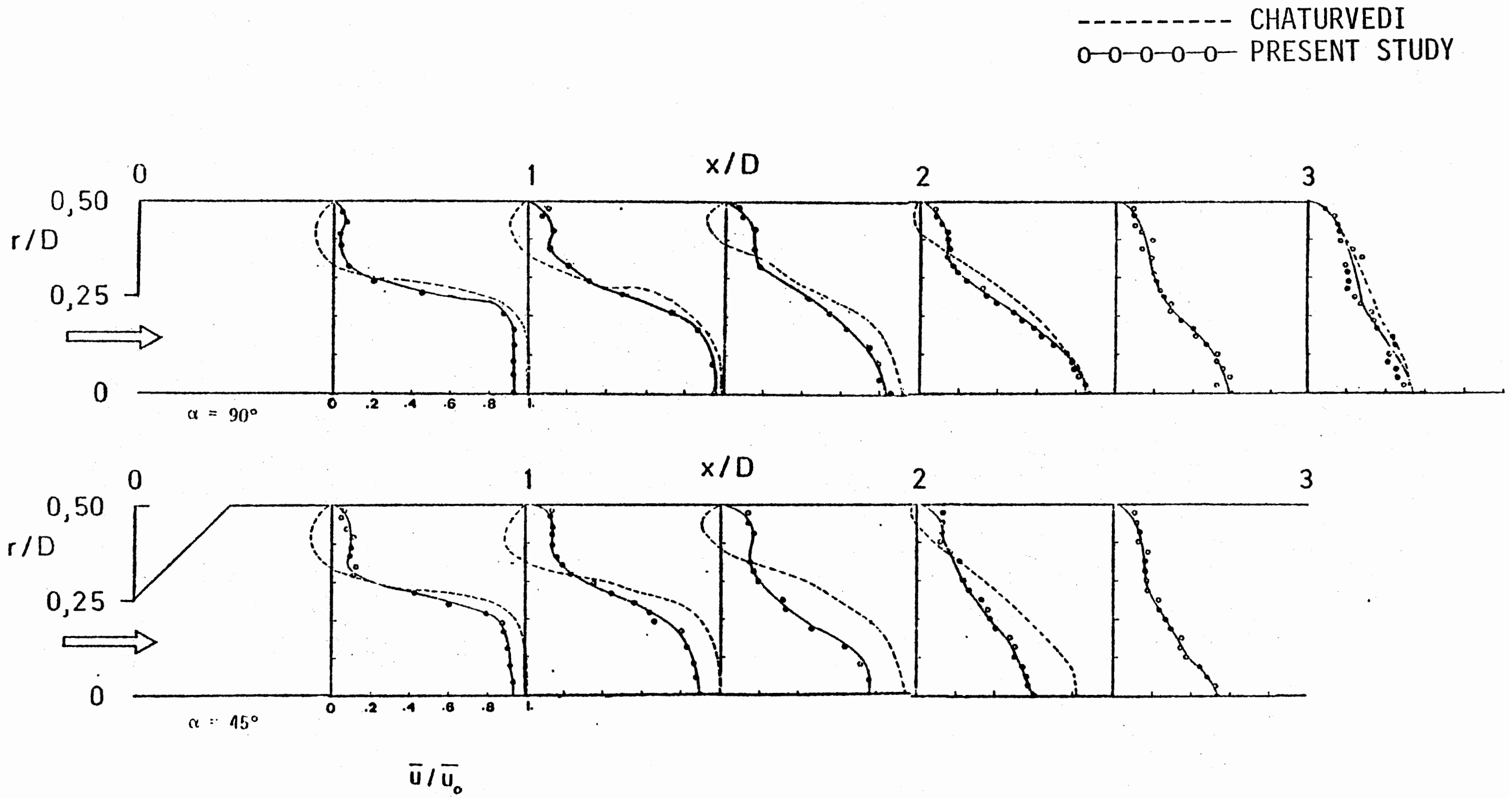

Figure 9. Radial Distribution of Normalized Time-Mean Axial Velocity in Nonswirling Confined Jet

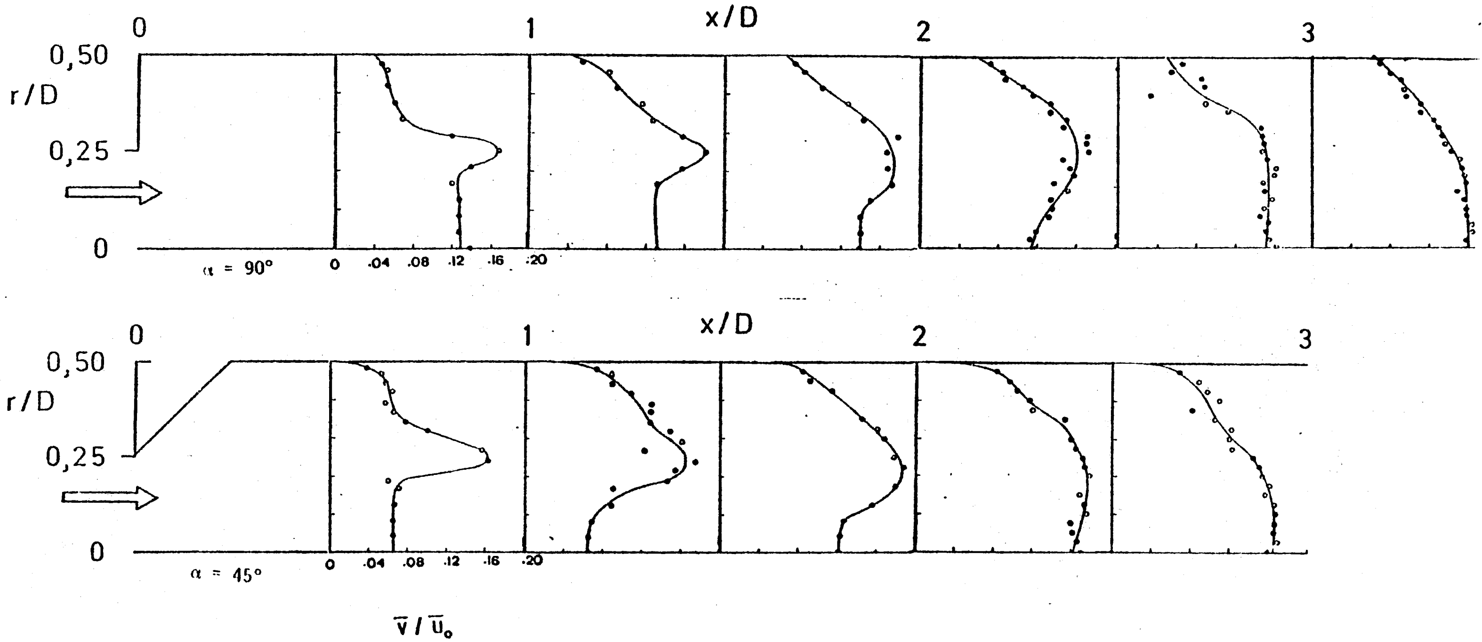

Figure 10. Radial Distribution of Normalized Time-Mean Radial Velocity in Nonswirling Confined Jet

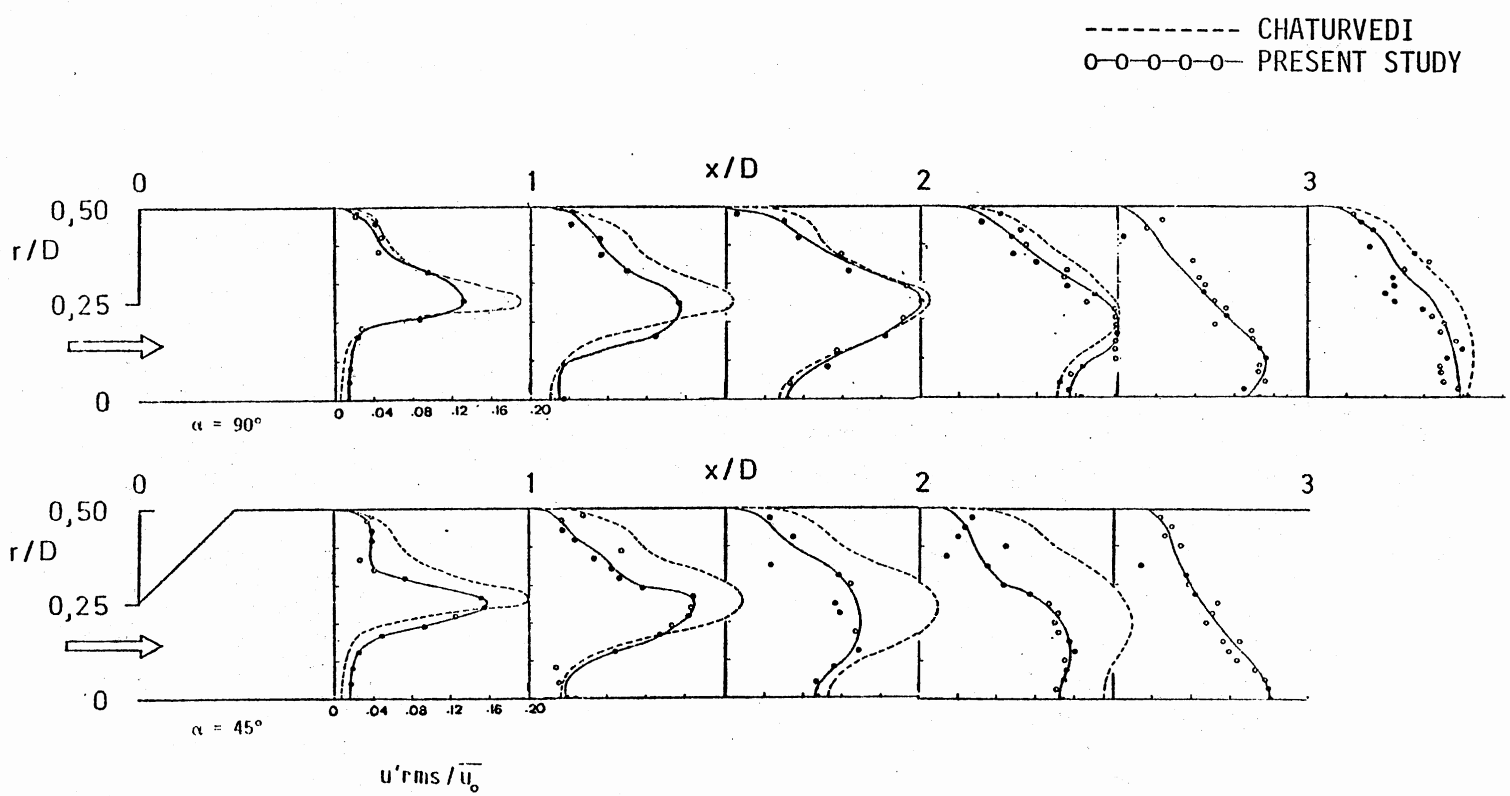

Figure 11. Radial Distribution of Axial Turbulence Intensity in Nonswirling Confined Jet

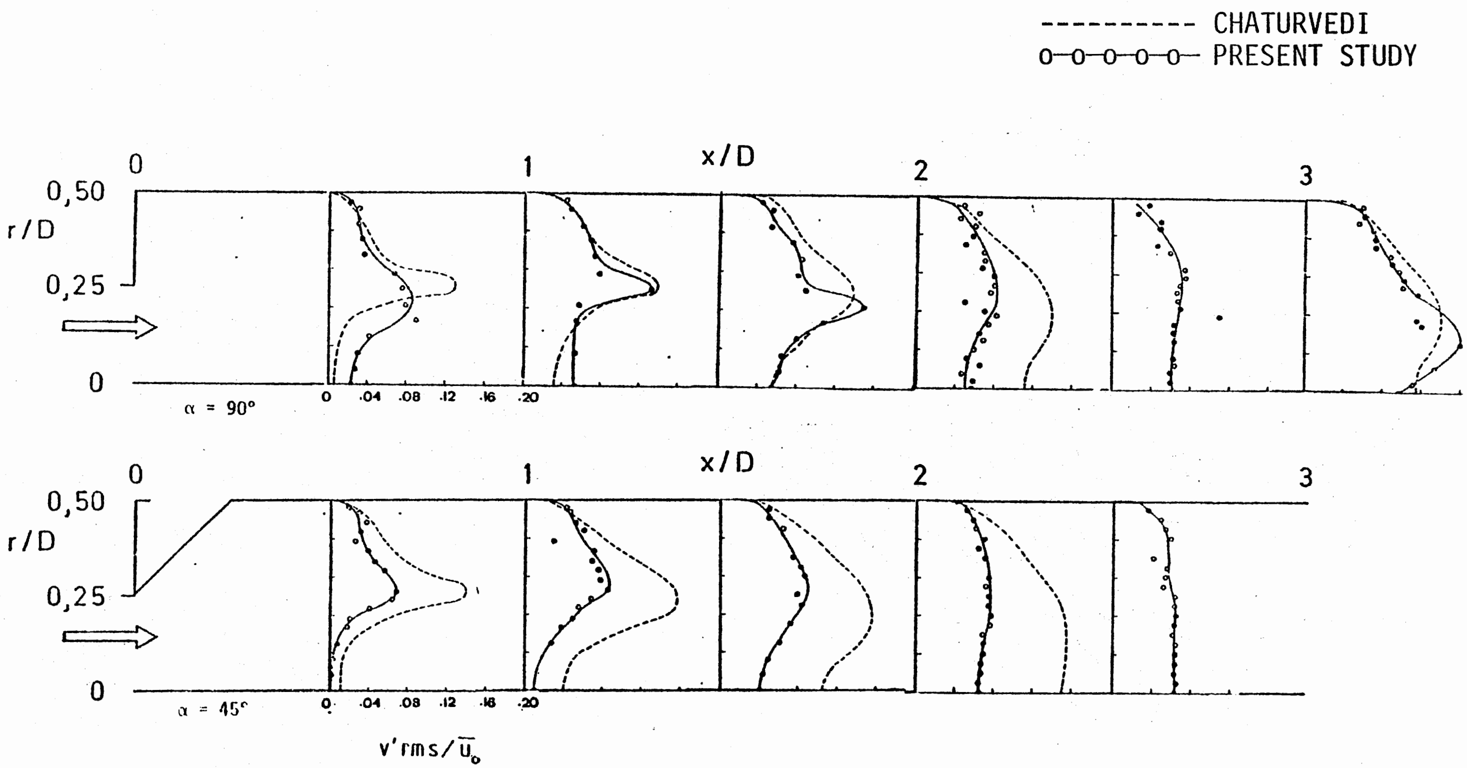

Figure 12. Radial Distribution of Radial Turbulence Intensity in Nonswirling Confined Jet

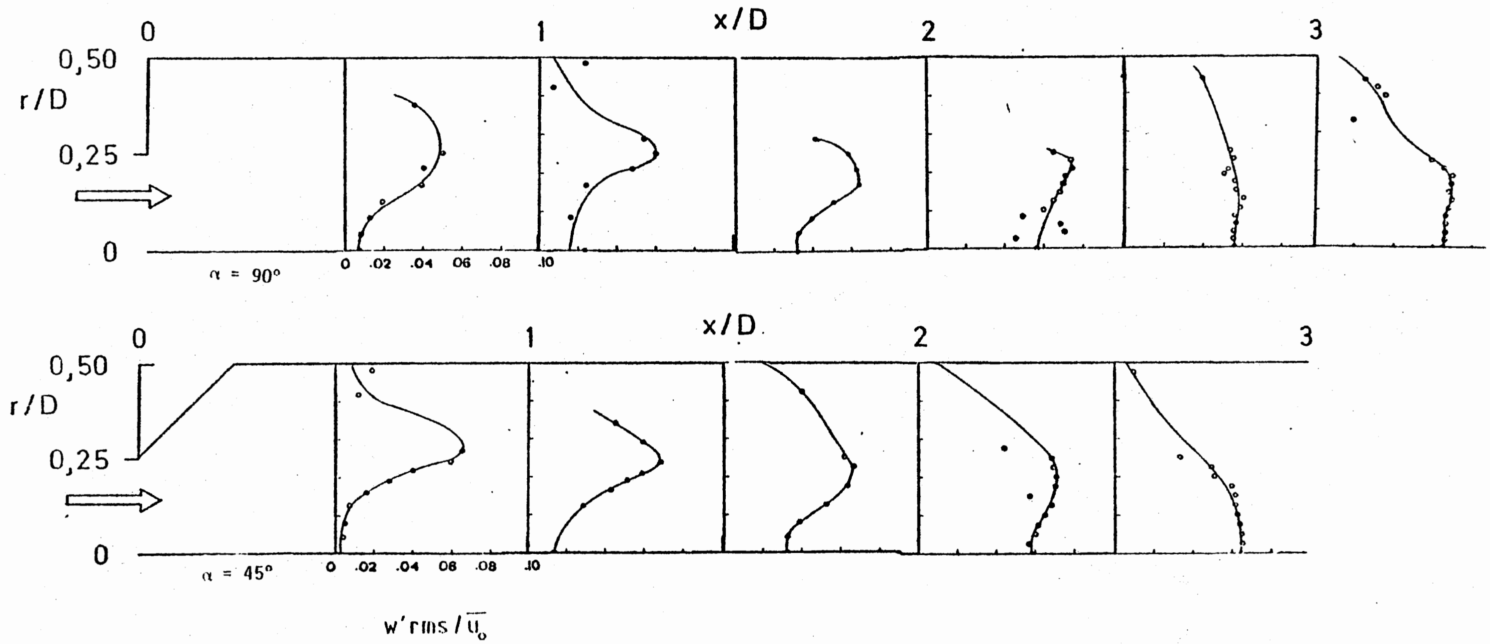

Figure 13. Radial Distribution of Azimuthal Turbulence Intensity in Nonswirling Confined Jet

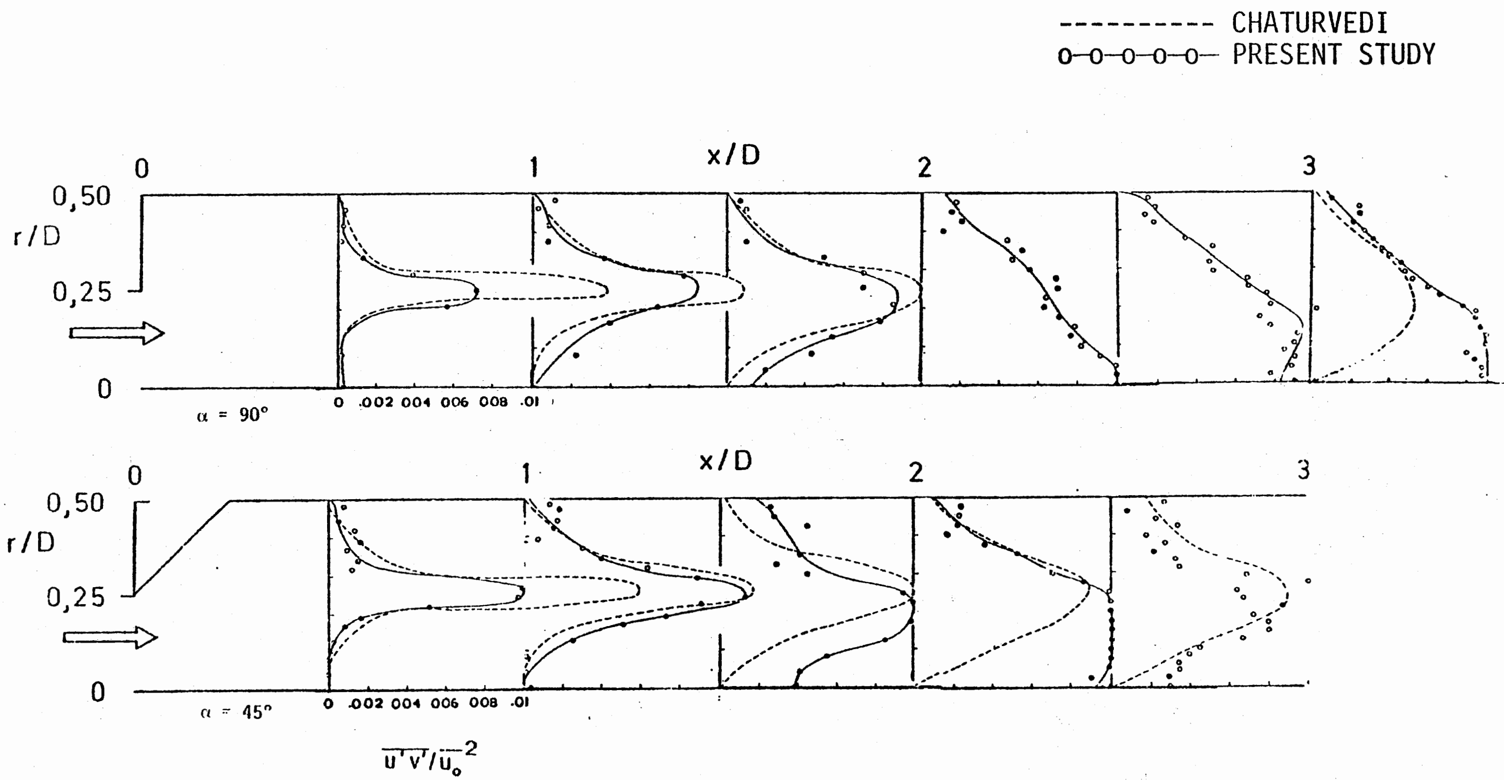

Figure 14. Radial Distribution of Shear Stress $\overline{u'v'}/\overline{u}_o^2$ in Nonswirling Confined Jet

APPENDIX C

USER'S GUIDE TO COMPUTER CODE FOR SIX-ORIENTATION HOT-WIRE DATA REDUCTION TECHNIQUE

USER'S GUIDE TO COMPUTER CODE FOR SIX-ORIENTATION HOT-WIRE DATA REDUCTION TECHNIQUE

A computer code is developed to obtain the turbulence quantities using the technique discussed in Chapter III. Measurements in a turbulent flowfield contain six mean and six root-mean-square voltages. A three-directional hot-wire calibration reveals three calibration constants in each direction. The input to the computer code is the mean, and root-mean-square voltages and also the calibration constants. The experimental data is then processed by the MAIN subprogram and various subroutines to get the output in the form of nine turbulence quantities consisting of the three mean velocities, the three turbulence intensities, and the three shear stresses. To facilitate the use of the computer code, the function of each subprogram is discussed here in detail.

1. The MAIN Subprogram

MAIN is the major part of the computer code which accepts the input in the form of mean and root-mean-square voltages and calibration constants and calls various subroutines to solve the equations listed in chapter III and finally calculates the turbulence quantities.

(8) Calculation of Mean Effective Cooling Velocities and Variances

Main calculates the six mean effective cooling velocities using Equation 14. This equation employs the input values of six mean voltages and calibration constants in $\hat{u}$-direction (see Figure 7, Appendix A). The MAIN then calculates the six values of variances using Equation 19. Equations 14 and 19 give mean and variance of individual cooling velocities in terms of the mean and variance of the appropriate voltage.

(ii) Calculation of Velocity Functions and Differentials

Having calculated the mean effective cooling velocities and variances, the MAIN then calls various subroutines to obtain the necessary information required to calculate velocity functions using Equations 9 through 11. The main then calculates the first and the second differentials of the three velocity functions with respect to the three selected mean effective cooling velocities. The differentials are given as:

$$\frac{\partial \overline{F1}}{\partial \overline{Z}_i} = \frac{\left[\dfrac{BO}{3(G^2 - K^2)^2}\,\dfrac{\partial BO}{\partial Z_i} + \dfrac{\overline{F1}^2}{(G^2 - K^2)}\,\dfrac{\partial AO}{\partial Z_i}\right]}{\left[2\overline{F1}^3 - 2F1\,\dfrac{AO}{(G^2 - K^2)}\right]} \tag{1}$$

$$\frac{\partial \overline{F2}}{\partial \overline{Z}_i} = \frac{\left[\dfrac{BO}{3\,(G^2 - K^2)^2}\,\dfrac{\partial BO}{\partial Z_i} - \dfrac{\overline{F2}^2}{(G^2 - K^2)^2}\,\dfrac{\partial AO}{\partial Z_i}\right]}{\left[2\,\overline{F2}^3 + \dfrac{2AO}{(G^2 - K^2)}\,\overline{F2}\right]} \tag{2}$$

$$\frac{\partial \overline{F3}}{\partial \overline{Z}_i} = \frac{\left[\dfrac{\partial CO}{\partial Z_i}\left\{\overline{F3}^2 - CO\right\} + \dfrac{(G^2 + K^2)}{(G^2 - K^2)}\left\{AO\,\dfrac{\partial Ao}{\partial Z_i} + \dfrac{BO}{3}\,\dfrac{\partial Bo}{\partial Z_i}\right\}\right]}{\left[2\overline{F3}^3 + 2CO\,\overline{F3}\right]} \tag{3}$$

$$\frac{\partial^2 \overline{F1}}{\partial \overline{Z}_i \partial \overline{Z}_j} = \frac{1}{2\left[\overline{F1}^3 - \dfrac{AO}{(G^2 - K^2)}\,\overline{F1}\right]} \left[-\left\{ 6\overline{F1}^2 - \frac{2AO}{(G^2 - K^2)} \right\} \frac{\partial \overline{F1}}{\partial \overline{Z}_i} \cdot \frac{\partial \overline{F1}}{\partial \overline{Z}_j} \right.$$

$$+ \frac{2\overline{F1}}{(G^2 - K^2)} \left\{ \frac{\partial \overline{F1}}{\partial \overline{Z}_i} \cdot \frac{\partial AO}{\partial \overline{Z}_j} + \frac{\partial AO}{\partial \overline{Z}_i} \cdot \frac{\partial \overline{F1}}{\partial \overline{Z}_j} \right\} + \frac{\overline{F1}^2}{(G^2 - K^2)} \cdot \frac{\partial^2 AO}{\partial \overline{Z}_i\, \partial \overline{Z}_j}$$

$$\left. + \frac{1}{3(G^2 - K^2)^2} \left\{ \frac{\partial BO}{\partial \overline{Z}_i} \cdot \frac{\partial BO}{\partial \overline{Z}_j} + BO\, \frac{\partial^2 BO}{\partial \overline{Z}_i\, \partial \overline{Z}_j} \right\} \right] \tag{4}$$

$$\frac{\partial^2 \overline{F2}}{\partial \overline{Z}_i\, \partial \overline{Z}_j} = \frac{1}{2\left[\overline{F2}^3 + \dfrac{AO}{(G^2 - K^2)}\,\overline{F2}\right]} \left[-\left\{ 6\overline{F2}^2 + \frac{2AO}{(G^2 - K^2)} \right\} \frac{\partial \overline{F2}}{\partial \overline{Z}_i} \cdot \frac{\partial \overline{F2}}{\partial \overline{Z}_j} \right.$$

$$- \frac{2\overline{F2}}{(G^2 - K^2)} \left\{ \frac{\partial \overline{F2}}{\partial Z_i} \cdot \frac{\partial AO}{\partial \overline{Z}_j} + \frac{\partial AO}{\partial \overline{Z}_i} \cdot \frac{\partial \overline{F2}}{\partial \overline{Z}_j} \right\} - \frac{\overline{F2}^2}{(G^2 - K^2)} \cdot \frac{\partial^2 AO}{\partial Z_i \partial Z_j}$$

$$\left. + \frac{1}{3(G^2 - K^2)^2} \left\{ \frac{\partial BO}{\partial Z_i} \cdot \frac{\partial BO}{\partial \overline{Z}_j} + BO\, \frac{\partial BO}{\partial Z_i \partial Z_j} \right\} \right] \tag{5}$$

$$\frac{\partial \overline{F3}}{\partial \overline{Z}_i \partial \overline{Z}_j} = \frac{1}{\left[2\overline{F3}^3 - 2CO \cdot \overline{F3}\right]} \cdot \left[-\left\{ 6\overline{F3}^2 - 2CO \right\} \cdot \frac{\partial \overline{F3}}{\partial \overline{Z}_i} \cdot \frac{\partial \overline{F3}}{\partial \overline{Z}_j} \right.$$

$$+ 2\overline{F3} \cdot \left\{ \frac{\partial \overline{F3}}{\partial \overline{Z}_i} \cdot \frac{\partial CO}{\partial \overline{Z}_j} + \frac{\partial CO}{\partial \overline{Z}_i} \cdot \frac{\partial \overline{F3}}{\partial \overline{Z}_j} \right\} - \frac{\partial CO}{\partial \overline{Z}_i} \cdot \frac{\partial CO}{\partial \overline{Z}_j}$$

$$+ \left\{ \overline{F3} - CO \right\} \frac{\partial^2 CO}{\partial \overline{Z}_i \partial \overline{Z}_j} + \frac{(G^2 + K^2)}{(G^2 - K^2)} \left\{ AO \cdot \frac{\partial AO}{\partial \overline{Z}_i \partial \overline{Z}_j} + \frac{\partial AO}{\partial Z_i} \cdot \frac{\partial AO}{\partial Z_j} \right.$$

$$\left.\left. + \frac{1}{3} \left(\frac{\partial BO}{\partial \overline{Z}_i} \cdot \frac{\partial BO}{\partial \overline{Z}_j} + BO\, \frac{\partial BO}{\partial \overline{Z}_i \partial \overline{Z}_j} \right) \right\} \right] \tag{6}$$

(iii) Calculation of Covariances

At this stage, the user has the option, whether to calculate the covariances by using King's (21) method or by assuming constant values of correlation coefficients. To get the covariances using King's method, the MAIN has to call the subroutine COVAR, otherwise MAIN calculates covariances using Equations 35, 41, and 44.

(iv) Calculation of the Turbulence Quantities

Now the MAIN has all the information needed to calculate the mean velocities using Equations 20 through 22, also to calculate the turbulence intensities using Equations 24 through 26, and finally to calculate the shear stresses using Equations 27 through 29. The MAIN then prints out the normalized values of the turbulence quantities in the form of nine two by three matrices each containing the six values of a turbulence quantity calculated using six different combinations.

2. Subroutine CPYF

This subroutine calculates the pitch and yaw factors using the calibration constants obtained by three-dimensional calibration. The equations used to calculate these factors are:

$$G = \frac{\hat{v}\ (\hat{w},\ \hat{u} = 0)}{\hat{u}\ (\hat{w},\ \hat{v} = 0)}$$

$$K = \frac{\hat{v}\ (\hat{w},\ \hat{u} = 0)}{\hat{w}\ (\hat{v},\ \hat{u} = 0)}$$

evaluated at a constant value of E^2. u, v, and w are obtained using equation 12 for their respective calibration constants. The value of E^2 can be adjusted to obtain an interval ΔE to get appropriate values of

G, and K.

3. Subroutine FMCV

The task of this subroutine is to find the mean effective cooling velocity which has minimum value among the six calculated by the MAIN. FMCV also finds the two mean effective cooling velocities which are adjacent to the minimum mean effective cooling velocity and returns the set of the three to be used by MAIN for further data processing.

4. Subroutine SEABC

SEABC recognizes the three selected mean effective cooling velocities Z_P, Z_Q, and Z_R, and sets the three appropriate equations for AO, BO, and CO in terms of $\overline{Z}_P$, $\overline{Z}_Q$, and $\overline{Z}_R$, using Table V. AO, BO, and CO, are used by MAIN to calculate the three velocity functions given by Equations 9 through 11.

5. Subroutine CDABC

CDABC calculates the first and second differentials of AO, BO, and CO with respect to $\overline{Z}_P$, $\overline{Z}_Q$, and $\overline{Z}_R$. It is evident from Table V that AO, BO, and CO are functions of $\overline{Z}_P$, $\overline{Z}_Q$, and $\overline{Z}_R$ and so are their first and second differentials.

6. Subroutine COVAR

This subroutine calculates covariances using a method suggested by King (21). This method calls for employing Equations 40 through 43. This subroutine can be called only when one desires to calculate covariances using King's method. Otherwise, the covariances are calculated within MAIN by the procedure already described.

TABLE V

LIST OF FORTRAN VARIABLES AND THEIR MEANING IN RESPONSE EQUATIONS

Input Values	
EM	$\overline{E}$
ER	E'rms
Mean Effective Cooling Velocities and Variances	
AMECV	$\overline{Z}$
VAR	$\sigma_Z{}^2$
Pitch and Yaw Factors	
PF	G
YF	K
Set of Three Cooling Velocities Chosen	
ZP	$\overline{Z}_P$
ZQ	$\overline{Z}_Q$
ZR	$\overline{Z}_R$
Derivatives of Functions A0, B0, and C0 (Definitions for B and C are analogous to those for A defined here)	
A1	$\frac{\partial A0}{\partial Z_P}$
A2	$\frac{\partial A0}{\partial Z_Q}$
A3	$\frac{\partial A0}{\partial Z_R}$
A21	$\frac{\partial^2 A0}{\partial Z_P{}^2}$
A22	$\frac{\partial^2 A0}{\partial Z_Q{}^2}$
A23	$\frac{\partial^2 A0}{\partial Z_R{}^2}$

TABLE V (Continued)

Derivatives of Velocity Functions F1, F2, and F3	
DF1P	$\frac{\partial \overline{F1}}{\partial Z_P}$
DF1Q	$\frac{\partial \overline{F1}}{\partial Z_Q}$
DF1R	$\frac{\partial \overline{F1}}{\partial Z_R}$
D2F1P	$\frac{\partial^2 \overline{F1}}{\partial {Z_P}^2}$
D2F1Q	$\frac{\partial^2 \overline{F1}}{\partial {Z_Q}^2}$
D2F1R	$\frac{\partial^2 \overline{F1}}{\partial {Z_R}^2}$
D2F1PQ	$\frac{\partial^2 \overline{F1}}{\partial Z_P \partial Z_Q}$
D2F1QR	$\frac{\partial^2 \overline{F1}}{\partial Z_Q \partial Z_R}$
D2F1PR	$\frac{\partial^2 \overline{F1}}{\partial Z_P \partial Z_R}$
Covariances	
AKPQ	$K_{Z_P Z_Q}$
AKQR	$K_{Z_Q Z_R}$
AKPR	$K_{Z_P Z_R}$

TABLE V (Continued)

Output Variables Calculated	
UMEAN	$\bar{u}$
WMEAN	$\bar{w}$
VMEAN	$\bar{v}$
UPRMS2	$\bar{u}'^2$
WPRMS2	$\bar{w}'^2$
VPRMS2	$\bar{v}'^2$
UVPB	$\overline{u'v'}$
UWPB	$\overline{u'w'}$
VWPB	$\overline{v'w'}$
UDUMO	$\bar{u}/\bar{u}_o$
WMDUMO	$\bar{w}/\bar{u}_o$
VMDUMO	$\bar{v}/\bar{u}_o$
UPDUMO	$\sqrt{\overline{u'^2}}/\bar{u}_o$
WPDUMO	$\sqrt{\overline{w'^2}}/\bar{u}_o$
VPDUMO	$\sqrt{\overline{v'^2}}/\bar{u}_o$
UVDUMO	$\overline{u'v'}/\bar{u}_o{}^2$
UWDUMO	$\overline{u'w'}/\bar{u}_o{}^2$
VWDUMO	$\overline{v'w'}/\bar{u}_o{}^2$

APPENDIX D

LISTING OF THE COMPUTER PROGRAM

```
C     ****************************************************************
C     *                                                              *
C     *                                                              *
C     *        COMPUTER PROGRAM TO CALCULATE TURBULENCE              *
C     *        QUANTITIES USING THE EXPERIMENTAL DATA                *
C     *        OBTAINED BY SIX ORIENTATION HOT-WIRE TECHNIQUE.       *
C     *                                                              *
C     *                                                              *
C     *                                                              *
C     *             VERSION OF OCT,1981                              *
C     *                                                              *
C     *                                                              *
C     *                                                              *
C     *                      PREPARED BY:                            *
C     *                    SALIM I. JANJUA                           *
C     *       SCHOOL OF MECHANICAL AND AEROSPACE ENGINEERING         *
C     *               OKLAHOMA STATE UNIVERSITY                      *
C     *                  STILLWATER OK. 74078                        *
C     *                                                              *
C     *                                                              *
C     ****************************************************************
C
C
C
C
      DIMENSION EM(12),ER(12),AMECV(12),VAR(12)
      DIMENSION UDUMO(6),UPDUMO(6),VMDUMO(6),VPDUMO(6)
      DIMENSION WMDUMO(6),WPDUMO(6),UVDUMO(6),UWDUMO(6),
     *VWDUMO(6)
      DATA DIA,EITA/12.0,0.8/
      REWIND 30
      NS=1
  908 IF(NS.EQ.0) GO TO 909
      READ(30,*) A,B,C
      READ(30,*) A1,B1,C1
      READ(30,*) A2,B2,C2
      WRITE(6,1111)
 1111 FORMAT(///,4X,'THE CALIBRATION CONSTANTS ARE:')
      WRITE(6,*) A,B,C
      WRITE(6,*) A1,B1,C1
      WRITE(6,*) A2,B2,C2
  909 READ(30,*, END=999) X,R,EMC,NS
      READ(30,*) (EM(I), I=1,6)
      READ(30,*) (ER(I), I=1,6)
      WRITE(6,1112)
 1112 FORMAT(///,9X,'THE MEAN AND R.M.S. VOLTAGES ARE:')
      WRITE(6,1100) (EM(I), I=1,6)
      WRITE(6,1200) (ER(I), I=1,6)
 1100 FORMAT(6F9.4)
 1200 FORMAT(6F9.4)
      RDDIA=R/DIA
      XDDIA=X/DIA
```

```
      UMO1=(-B+SQRT(B**2-4.0*C*(A-EMO**2)))/(2.0*C)
      UM1=(-B+SQRT(B**2-4.0*C*(A-EM(1)**2)))/(2.0*C)
      UMO=UMO1*UMO1
      UM=UM1*UM1
      DEU=B/(4.0*EM(1)*UM1)+C/(2.0*EM(1))
      UDEU=UM*DEU
      UPDUM=ER(1)/UDEU
      UMDUMO=UM/UMO
      UPDUMM=UPDUM*UMDUMO
      DO 30 I=1,6
      EM2=EM(I)*EM(I)
      ER2=ER(I)*ER(I)
      D=SQRT(B**2-(4*C*(A-EM2)))
      PHE=((-B+D)/(2*C))**2
      DPHE=(2*EM(I)/C)*(1-(B/D))
      D2PHE=(1/EM(I))*DPHE+(8*B*EM2)/D**3
C-------------------------------------------------------------
C-------------LOCAL MEAN EFFECTIVE COOLING VELOCITY IS CALCULATED
C-------------------------------------------------------------
      AMECV(I)=PHE+0.5*D2PHE*ER2
C-------------------------------------------------------------
C--------------VARIANCE,VAR IS CALCULATED--------------
C-------------------------------------------------------------
      VAR(I)=((DPHE**2)*(ER2))-((0.5*D2PHE*ER2)**2)
      AMECV(I+6)=AMECV(I)
      VAR(I+6)=VAR(I)
      WRITE(6,112)
      WRITE(6,110) AMECV(I),VAR(I)
  110 FORMAT(//,7X,'AMECV=',F7.4,5X,'VAR=',F7.4)
   30 CONTINUE
C-------------------------------------------------------------
C--------------MAIN CALLS THE SUBROUTINE CPYF TO CALCULATE
C--------------THE PITCH AND YAW FACTORS.------------------
C-------------------------------------------------------------
      CALL CPYF(A,B,C,A1,B1,C1,A2,B2,C2,PF,YF)
C-------------------------------------------------------------
C-----------PITCH FACTOR AND YAW FACTOR---------------------
C-------------------------------------------------------------
      WRITE(6,543) PF,YF
  543 FORMAT(///,7X,'PITCH FACTOR=',F7.4,3X,'YAW FACTOR=',F7.4)
      AL=PF*PF-YF*YF
      O=PF*PF+YF*YF
      WRITE(6,444) UMDUMO,UPDUMM
  444 FORMAT(///,7X,'AXIAL MEAN VEL/INLET MAX VEL=',F8.4,4X,
     *'AXIAL TURB INTEN=',F8.4)
      WRITE(6,515) UMO
  515 FORMAT(//,12X,'MAX INLET VELOCITY=',F9.4)
      DO 222 III=1,6
      II=III-1
      N=50
      CALL STOTZ(UDUMO,WMDUMO,VMDUMO,UPDUMO,WPDUMO,VPDUMO,
     *UVDUMO,UWDUMO,VWDUMO,N,III)
C-------------------------------------------------------------
C-----------------MAIN CALLS THE  SUBROUTINE FMCV TO FIND THE
C-----------------THE MINIMUM COOLING VELOCITY AND THE TWO
C-----------------ADJACENT ONES
C-------------------------------------------------------------
```

```
      CALL FMCV(AMECV,N,IP,IQ,IR,II)
      ZP=AMECV(IP)
      ZQ=AMECV(IQ)
      ZR=AMECV(IR)
      IF(IQ.GT.6) IQ=IQ-6
      IF(IR.GT.6) IR=IR-6
C-----------------------------------------------------------
C-----------------MAIN CALLS THE SUBROUTINE,SEABC TO SET UP
C-----------------THE EQUATIONS FOR AO,BO,AND CO-----------
C----------------------------------------------------------
      CALL SEABC(ZP,ZQ,ZR,IP,AO,BO,CO)
      F=SQRT((AO**2)+(BO**2)/3)
      IF(CO.LT.F*O/AL) GO TO 222
C-----------------------------------------------------------
C--------------VELOCITY FUNCTIONS F1,F2,AND F3 ARE CALCULATED-----
C----------------------------------------------------------------
      F1=SQRT((1/AL)*(AO+F))
      IF((1/AL)*(-AO+F).LT.0) GO TO 222
      F2=SQRT((1/AL)*(-AO+F))
      F3=SQRT(CO-(O/AL)*F)
      IF(F2.EQ.0) GO TO 222
C-----------------------------------------------------------
C---------------MAIN CALLS THE SUBROUTINE CDABC TO CALCULATE
C---------------THE FIRST AND SECOND DIFFERENTIALS OF AO,BO,
C---------------AND CO-------------------------------------------
C-----------------------------------------------------------
      CALL CDABC(DAP,DBP,DCP,D2AP,D2BP,D2CP,DAQ,DBQ,DCQ,D2AQ,D2BQ,
     *D2CQ,DAR,DBR,DCR,D2AR,D2BR,D2CR,ZP,ZQ,ZR,IP)
C-------------------MAIN CALCULATES THE FIRST AND SECOND
C-------------------DIFFERENTIALS OF THE VELOCITY FUNCTIONS
C-------------------F1,F2,AND F3 WITH RESPECT TO THE
C-------------------SELECTED SET OF THREE COOLING VELO
C-------------------CITIES.---------------------------------
C-----------------------------------------------------------
      X1=F1*F1
      X2=X1*F1
      X3=BO/(3*AL*AL)
      X4=X1/AL
      X5=(2*X2)-(2*F1*AO/AL)
      X6=-(6*X1-2*AO/AL)
      Y1=F2*F2
      Y2=Y1*F2
      Y3=2.0*Y2+2.0*F2*AO/AL
      Y4=Y1/AL
      Y5=-(6*Y1+(2.0*AO/AL))
      Z1=F3*F3
      Z2=Z1*F3
      Z3=2.0*Z2-2.0*CO*F3
      Z4=-(6.0*Z1-2.0*CO)
      DF1P=(X3*DBP+X4*DAP)/X5
      DF2P=(X3*DBP-Y4*DAP)/Y3
      DF3P=(DCP*(Z1-CO)+((O*O)/(AL*AL))*(AO*DAP+(BO*DBP)/3))/Z3
      DF1Q=(X3*DBQ+X4*DAQ)/X5
      DF2Q=(X3*DBQ-Y4*DAQ)/Y3
      DF3Q=(DCQ*(Z1-CO)+((O*O)/(AL*AL))*(AO*DAQ+(BO*DBQ)/3))/Z3
      DF1R=(X3*DBR+X4*DAR)/X5
      DF2R=(X3*DBR-Y4*DAR)/Y3
```

```
      DF3P=(DCP*(Z1-CO)+((O*O)/(AL*AL))*(AO*DAP+(BO*DBP)/3))/Z3
       D2F1P=((X6*DF1P*DF1P)+(2.0*F1/AL)*(DAP*DF1P+DAP*DF1P)+(D2AP
     **X1/AL)+(1/(3*AL*AL))*(DBP*DBP+BO*D2BP))/X5
       D2F2P=((Y5*DF2P*DF2P)-(2.0*F2/AL)*(DF2P*DAP+DAP*DF2P)-(Y1*D2
     *AP/AL)+(DBP*DBP+BO*D2BP)/(3.0*AL*AL))/Y3
       D2F3P=((Z4*DF3P*DF3P)+2*F3*(DF3P*DCP+DCP*DF3P)-(DCP*DCP)+(Z1
     *-CO)*D2CP+((O*O)/(AL*AL))*((AO*D2AP+DAP*DAP)+(DBP*DBP
     *+BO*D2BP)/3))/Z3
       D2F1Q=((X6*DF1Q*DF1Q)+(2.0*F1/AL)*(DAQ*DF1Q+DAQ*DF1Q)+(D2AQ
     **X1/AL)+(1/(3.0*AL*AL))*(DBQ*DBQ+BO*D2BQ))/X5
       D2F2Q=((Y5*DF2Q*DF2Q)-(2.0*F2/AL)*(DF2Q*DAQ+DAQ*DF2Q)-(Y1*D
     *2AQ/AL)+(DBQ*DBQ+BO*D2BQ)/(3.0*AL*AL))/Y3
       D2F3Q=((Z4*DF3Q*DF3Q)+2.0*F3*(DF3Q*DCQ+DCQ*DF3Q)-(DCQ*DCQ)
     *+(Z1-CO)*D2CQ+((O*O)/(AL*AL))*((AO*D2AQ+DAQ*DAQ)+(
     *DBQ*DBQ+BO*D2BQ)/3))/Z3
       D2F1R=((X6*DF1R*DF1R)+(2.0*F1/AL)*(DAR*DF1R+DAR*DF1R)+(D2AR
     **X1/AL)+(1/(3.0*AL*AL))*(DBR*DBR+BO*D2BR))/X5
       D2F2R=((Y5*DF2R*DF2R)-(2.0*F2/AL)*(DF2R*DAR+DAR*DF2R)-(Y1*D
     *2AR/AL)+(DBR*DBR+BO*D2BR)/(3.0*AL*AL))/Y3
       D2F3R=((Z4*DF3R*DF3R)+2.0*F3*(DF3R*DCR+DCR*DF3R)-(DCR*DCR)
     *+(Z1-CO)*D2CR+((O*O)/(AL*AL))*((AO*D2AR+DAR*DAR)+(
     *DBR*DBR+BO*D2BR)/3))/Z3
       D2F1PQ=((X6*DF1P*DF1Q)+(2.0*F1/AL)*(DAP*DF1Q+DAQ*DF1P)+(X1
     **D2APQ/AL)+(1/(3.0*AL*AL))*(DBP*DBQ+BO*D2BPQ))/X5
       D2F1QR=((X6*DF1Q*DF1R)+(2.0*F1/AL)*(DAQ*DF1R+DAR*DF1Q)+(X1
     **D2AQR/AL)+(1/(3.0*AL*AL))*(DBQ*DBR+BO*D2BQR))/X5
       D2F1PR=((X6*DF1P*DF1R)+(2.0*F1/AL)*(DAP*DF1R+DAR*DF1P)+(X1
     **D2APR/AL)+(1/(3.0*AL*AL))*(DBP*DBR+BO*D2BPR))/X5
       D2F2PQ=((Y5*D2FP*D2FQ)-(2.0*F2/AL)*(DF2P*DAQ+DAP*DF2Q)-(Y1
     **D2APQ/AL)+(1/(3.0*AL*AL))*(DBP*DBQ+BO*D2BPQ))/Y3
       D2F2QR=((Y5*DF2Q*DF2R)-(2.0*F2/AL)*(DF2Q*DAR+DAQ*DF2R)-(Y1
     **D2AQR/AL)+(1/(3.0*AL*AL))*(DBQ*DBR+BO*D2BQR))/Y3
       D2F2PR=((Y5*DF2P*DF2R)-(2.0*F2/AL)*(DF2P*DAR+DAP*DF2R)-(Y1
     **D2APR/AL)+(1/(3.0*AL*AL))*(DBP*DBP+BO*D2BPR))/Y3
       D2F3PQ=((Z4*DF3P*DF3Q)+2.0*F3*(DF3P*DCQ+DCP*DF3Q)-(DCP*DCQ)
     *+(Z1-CO)*D2CPQ+((O*O)/(AL*AL))*((AO*D2APQ+DAP*DAQ)+(
     *DBP*DBQ+BO*D2BPQ)/3))/Z3
       D2F3QR=((Z4*DF3Q*DF3R)+2.0*F3*(DF3Q*DCR+DCQ*DF3R)-(DCQ*DCR)
     *+(Z1-CO)*D2CQR+((O*O)/(AL*AL))*((AO*D2AQR+DAQ*DAR)+(
     *DBQ*DBR+BO*D2BQR)/3))/Z3
       D2F3PR=((Z4*DF3P*DF3R)+2.0*F3*(DF3P*DCR+DCP*DF3R)-(DCP*DCR)
     *+(Z1-CO)*D2CPR+((O*O)/(AL*AL))*((AO*D2APR+DAP*DAR)+(
     *DBP*DBR+BO*D2BPR)/3))/Z3
C-------------------------------------------------------------
C---------------------MAIN CALLS THE SUBROUTINE COVAR TO
C-----------------------CALCULATE THE COVARIANCE BETWEEN THE
C-----------------------SELECTED COOLING VELOCITIES.-------
C----------------------------------------------------------
       AKPQ=0.9*SQRT(VAR(IP)*VAR(IP+1))
       AKQR=0.9*SQRT(VAR(IP+1)*VAR(IP+2))
       AKPR=0.81*EITA*SQRT(VAR(IP)*VAR(IP+2))
       AKQP=AKPQ
       AKRQ=AKQR
       AKRP=AKPR
C-------------------------------------------------------------
C---------------------MAIN CALCULATES THE AXIAL,RADIAL,AND
C---------------------TANGENTIAL MEAN VELOCITIES.-----------
```

```
C-------------------------------------------------------------
      UMEAN=F1+0.5*(D2F1P*VAR(IP)+D2F1Q*VAR(IP+1)+D2F1R*VAR(IP+2))
     *+D2F1PQ*AKPQ+D2F1QR*AKQR+D2F1PR*AKPR
      WMEAN=F2+0.5*(D2F2P*VAR(IP)+D2F2Q*VAR(IP+1)+D2F2R*VAR(IP+2))
     *+D2F2PQ*AKPQ+D2F2QR*AKQR+D2F2PR*AKPR
      VMEAN=F3+0.5*(D2F3P*VAR(IP)+D2F3Q*VAR(IP+1)+D2F3R*VAR(IP+2))
     *+D2F3PQ*AKPQ+D2F3QR*AKQR+D2F3PR*AKPR
      UP1=DF1P*DF1P*VAR(IP)+DF1Q*DF1Q*VAR(IP+1)+DF1R*DF1R*VAR(IP
     *+2)
      UP2=DF1P*DF1Q*AKPQ+DF1P*DF1R*AKPR+DF1Q*DF1P*AKQP+DF1Q*DF1R*A
     *KQR+DF1R*DF1P*AKRP+DF1R*DF1Q*AKRQ
      UP3=0.5*(D2F1P*VAR(IP)+D2F1Q*VAR(IP+1)+D2F1R*VAR(IP+2))
      UP4=D2F1PQ*AKPQ+D2F1QR*AKQR+D2F1PR*AKPR
      UP5=UP3+UP4
      UPRMS2=UP1+UP2-UP5**2
      WP1=DF2P*DF2P*VAR(IP)+DF2Q*DF2Q*VAR(IP+1)+DF2R*DF2R*VAR(IP
     *+2)
      WP2=DF2P*DF2Q*AKPQ+DF2P*DF2R*AKPR+DF2Q*DF2P*AKQP+DF2Q*DF2R*A
     *KQR+DF2R*DF2P*AKRP+DF2R*DF2Q*AKRQ
      WP3=0.5*(D2F2P*VAR(IP)+D2F2Q*VAR(IP+1)+D2F2R*VAR(IP+2))
      WP4=D2F2PQ*AKPQ+D2F2QR*AKQR+D2F2PR*AKPR
      WP5=WP3+WP4
      WPRMS2=WP1+WP2-WP5**2
      VP1=DF3P*DF3P*VAR(IP)+DF3Q*DF3Q*VAR(IP+1)+DF3R*DF3R*VAR(IP
     *+2)
      VP2=DF3P*DF3Q*AKPQ+DF3P*DF3R*AKPR+DF3Q*DF3P*AKQP+DF3Q*DF3R*A
     *KQR+DF3R*DF3P*AKRP+DF3R*DF3Q*AKRQ
      VP3=0.5*(D2F3P*VAR(IP)+D2F3Q*VAR(IP+1)+D2F3R*VAR(IP+2))
      VP4=D2F3PQ*AKPQ+D2F3QR*AKQR+D2F3PR*AKPR
      VP5=VP3+VP4
      VPRMS2=VP1+VP2-VP5**2
      UV1=DF1P*DF3P*VAR(IP)+DF1Q*DF3Q*VAR(IP+1)+DF1R*DF3R*VAR(IP
     *+2)
      UV2=DF1P*DF3Q*AKPQ+DF1P*DF3R*AKPR+DF1Q*DF3P*AKQP+DF1Q*DF3R*A
     *KQR+DF1R*DF3P*AKRP+DF1R*DF3Q*AKRQ
      UV3=0.5*(D2F1P*VAR(IP)+D2F1Q*VAR(IP+1)+D2F1R*VAR(IP+2))
      UV4=D2F1PQ*AKPQ+D2F1QR*AKQR+D2F1PR*AKPR
      UV5=0.5*(D2F3P*VAR(IP)+D2F3Q*VAR(IP+1)+D2F3R*VAR(IP+1))
      UV6=D2F3PQ*AKPQ+D2F3QR*AKQR+D2F3PR*AKPR
      UVPB=UV1+UV2-((UV3+UV4)*(UV5+UV6))
      VW1=DF3P*DF2P*VAR(IP)+DF3Q*DF2Q*VAR(IP+1)+DF3R*DF2R*VAR(IP
     *+2)
      VW2=DF3P*DF2Q*AKPQ+DF3P*DF2R*AKPR+DF3Q*DF2P*AKQP+DF3Q*DF2R*A
     *KQR+DF3R*DF2P*AKRP+DF3R*DF2Q*AKRQ
      VW3=0.5*(D2F3P*VAR(IP)+D2F3Q*VAR(IP+1)+D2F3R*VAR(IP+2))
      VW4=D2F3PQ*AKPQ+D2F3QR*AKQR+D2F3PR*AKPR
      VW5=0.5*(D2F2P*VAR(IP)+D2F2Q*VAR(IP+1)+D2F2R*VAR(IP+1))
      VW6=D2F2PQ*AKPQ+D2F2QR*AKQR+D2F2PR*AKPR
      VWPB=VW1+VW2-((VW3+VW4)*(VW5+VW6))
      UW1=DF1P*DF2P*VAR(IP)+DF1Q*DF2Q*VAR(IP+1)+DF1R*DF2R*VAR(IP
     *+2)
      UW2=DF1P*DF2Q*AKPQ+DF1P*DF2R*AKPR+DF1Q*DF2P*AKQP+DF1Q*DF2R*A
     *KQR+DF1R*DF2P*AKRP+DF1R*DF2Q*AKRQ
      UW3=0.5*(D2F1P*VAR(IP)+D2F1Q*VAR(IP+1)+D2F1R*VAR(IP+2))
      UW4=D2F1PQ*AKPQ+D2F1QR*AKQR+D2F1PR*AKPR
      UW5=0.5*(D2F2P*VAR(IP)+D2F2Q*VAR(IP+1)+D2F2R*VAR(IP+1))
      UW6=D2F2PQ*AKPQ+D2F2QR*AKQR+D2F2PR*AKPR
```

```
      UWPP=UW1+UW2-((UW3+UW4)*(UW5+UW6))
      UDUMO(I11)=UMEAN/UMO
      WMDUMO(I11)=WMEAN/UMO
      VMDUMO(I11)=VMEAN/UMO
      IF(UPRMS2.GT.0.0) UPDUMO(I11)=SQRT(UPRMS2)/UMO
      IF(WPRMS2.GT.0.0) WPDUMO(I11)=SQRT(WPRMS2)/UMO
      IF(VPRMS2.GT.0.0) VPDUMO(I11)=SQRT(VPRMS2)/UMO
      UVDUMO(I11)=UVPB/UMO**2
      VWDUMO(I11)=VWPB/UMO**2
      UWDUMO(I11)=UWPB/UMO**2
  112 FORMAT('        ')
  222 CONTINUE
      WRITE(6,113) RODIA
      WRITE(6,114) XODIA
  114 FORMAT(///,20X,'AXIAL DISTANCE X/D=',F7.3)
  113 FORMAT(//,20X,'RADIAL DISTANCE R/D=',F5.4)
      WRITE(6,112)
      WRITE(6,112)
      WRITE(6,1000) (UDUMO(I),I=1,3)
      WRITE(6,1000) (UDUMO(I),I=4,6)
      WRITE(6,112)
      WRITE(6,112)
      WRITE(6,2000) (WMDUMO(I),I=1,3)
      WRITE(6,2000) (WMDUMO(I),I=4,6)
      WRITE(6,112)
      WRITE(6,112)
      WRITE(6,3000) (VMDUMO(I),I=1,3)
      WRITE(6,3000) (VMDUMO(I),I=4,6)
      WRITE(6,112)
      WRITE(6,112)
      WRITE(6,4000) (UPDUMO(I),I=1,3)
      WRITE(6,4000) (UPDUMO(I),I=4,6)
      WRITE(6,112)
      WRITE(6,112)
      WRITE(6,5000) (WPDUMO(I),I=1,3)
      WRITE(6,5000) (WPDUMO(I),I=4,6)
      WRITE(6,112)
      WRITE(6,112)
      WRITE(6,6000) (VPDUMO(I),I=1,3)
      WRITE(6,6000) (VPDUMO(I),I=4,6)
      WRITE(6,112)
      WRITE(6,112)
      WRITE(6,7000) (UVDUMO(I),I=1,3)
      WRITE(6,7000) (UVDUMO(I),I=4,6)
      WRITE(6,112)
      WRITE(6,112)
      WRITE(6,8000) (UWDUMO(I),I=1,3)
      WRITE(6,8000) (UWDUMO(I),I=4,6)
      WRITE(6,112)
      WRITE(6,112)
      WRITE(6,112)
      WRITE(6,9000) (VWDUMO(I),I=1,3)
      WRITE(6,9000) (VWDUMO(I),I=4,6)
      WRITE(6,112)
      WRITE(6,112)
 1000 FORMAT(/,7X,'UDUMO=',F9.4,5X,'UDUMO=',F9.4,5X,'UDUMO=',
     *F9.4)
```

```
 2000 FORMAT(/,7X,'WDUMO=',F9.4,5X,'WDUMC=',F9.4,5X,'WDUMO=',
     *F9.4)
 3000 FORMAT(/,7X,'VDUMC=',F9.4,5X,'VDUMC=',F9.4,5X,'VDUMO=',
     *F9.4)
 4000 FORMAT(/,7X,'UPDUMC=',F9.4,4X,'UPDUMO=',F9.4,4X,'UPDUMO'
     *,'=',F9.4)
 5000 FORMAT(/,7X,'WPDUMO=',F9.4,4X,'WPDUMO=',F9.4,4X,'WPDUMO'
     *,'=',F9.4)
 6000 FORMAT(/,7X,'VPDUMC=',F9.4,4X,'VPDUMO=',F9.4,4X,'VPDUMC'
     *,'=',F9.4)
 7000 FORMAT(/,7X,'UVDUMC=',F9.4,4X,'UVDUMC=',F9.4,4X,'UVDUMO='
     *,F9.4)
 8000 FORMAT(/,7X,'UWDUMO=',F9.4,4X,'UWDUMC=',F9.4,4X,'UWDUMO='
     *,F9.4)
 9000 FORMAT(/,7X,'VWDUMC=',F9.4,4X,'VWDUMO=',F9.4,4X,'VWDUMC='
     *,F9.4)
      GO TO 908
  999 STOP
      END


C
C
C
C
C
C******************************************************************
C-----------THIS SUBROUTINE SETS TURBULENT QUANTITIES TO
C-----------ZERO AT THE BEGINING OF EACH ITERATION
C******************************************************************
      SUBROUTINE STOTZ(UDUMC,WMDUMO,VMDUMC,UPDUMO,WPDUMO,
     *VPDUMC,UVDUMC,UWDUMC,VWDUMC,N,I)
      DIMENSION UDUMO(6),WMDUMO(6),VMDUMO(6),UPDUMO(6),WPDUMO(6)
      DIMENSION VPDUMO(6),UVDUMO(6),UWDUMC(6),VWDUMO(6)
      UDUMO(I)=0.0
      WMDUMO(I)=0.0
      VMDUMC(I)=0.0
      UPDUMO(I)=0.0
      WPDUMC(I)=0.0
      VPDUMC(I)=0.0
      UVDUMC(I)=0.0
      UWDUMC(I)=0.0
      VWDUMC(I)=0.0
      RETURN
      END
```

```
C
C
C
C*****************************************************************
C
C     THIS SUBROUTINE FINDS THE MINIMUM MEAN EFFECTIVE
C     COOLING VELOCITY AND THE TWO ADJACENT TO IT.
C
C*****************************************************************
C
C
C
C
      SUBROUTINE FMCV(CV,N,IX,IY,IZ,II)
      DIMENSION CV(50)
      IF(CV(2).LT.CV(1)) GO TO 20
      IF(CV(3).LT.CV(1)) GO TO 30
      IF(CV(4).LT.CV(1)) GO TO 40
      IF(CV(5).LT.CV(1)) GO TO 50
      IF(CV(6).LT.CV(1)) GO TO 60
      IX=6
      IY=1
      IZ=2
      GO TO 100
   20 IF(CV(3).LT.CV(2)) GO TO 30
      IF(CV(4).LT.CV(2)) GO TO 40
      IF(CV(5).LT.CV(2)) GO TO 50
      IF(CV(6).LT.CV(2)) GO TO 60
      IX=1
      IY=2
      IZ=3
      GO TO 100
   30 IF(CV(4).LT.CV(3)) GO TO 40
      IF(CV(5).LT.CV(3)) GO TO 50
      IF(CV(6).LT.CV(3)) GO TO 60
      IX=2
      IY=3
      IZ=4
      GO TO 100
   40 IF(CV(5).LT.CV(4)) GO TO 50
      IF(CV(6).LT.CV(4)) GO TO 60
      IX=3
      IY=4
      IZ=5
      GO TO 100
   50 IF(CV(6).LT.CV(5)) GO TO 60
      IX=4
      IY=5
      IZ=6
      GO TO 100
   60 IX=5
      IY=6
      IZ=1
  100 IX=IX+II
      IF(IX.GT.6) IX=IX-6
      IF(IY.GT.6) IY=IY-6
      IF(IZ.GT.6) IZ=IZ-6
      IY=IX+1
      IZ=IX+2
      RETURN
      END
```

```
C
C*************************************************************
C
C      THIS SUBROUTINE CALCULATES THE PITCH AND YAW
C      FACTORS USING THE THREE-DIRECTIONAL CALIBRATION
C      CONSTANTS.
C
C*************************************************************
C
       SUBROUTINE CPYF(A,B,C,A1,B1,C1,A2,B2,C2,PF,YF)
       E=3.0
   10  W1=B1**2-4.0*C1*(A1-E**2)
       IF(W1.LT.0.0) GO TO 20
       E=E+0.05
       GO TO 10
   20  E=E-0.05
       W1=(-B1+SQRT(B1**2-4.0*C1*(A1-E**2)))/(2.0*C1)
       W=W1*W1
       V1=(-B2-SQRT(B2**2-4.0*C2*(A2-E**2)))/(2.0*C2)
       V=V1*V1
       U1=(-B+SQRT(B**2-4.0*C*(A-E**2)))/(2.0*C)
       U=U1*U1
       PF=V/U
       YF=V/W
       RETURN
       END
C*************************************************************
C
C      THIS SUBROUTINE SETS EQUATIONS FOR AC,BC,AND CO
C      DEPENDING UPON THE SET OF THE THREE COOLING
C      VELOCITIES CHOSEN.
C
C*************************************************************
C
       SUBROUTINE SEABC(A1,A2,A3,K,X,Y,Z)
       IF(K.EQ.1) GO TO 15
       IF(K.EQ.2) GO TO 25
       IF(K.EQ.3) GO TO 35
       IF(K.EQ.4) GO TO 45
       IF(K.EQ.5) GO TO 55
       IF(K.EQ.6) GO TO 65
   15  X=A2**2-A3**2
       Y=-2.0*A1**2+3.0*A2**2-A3**2
       Z=A1**2-A2**2+A3**2
       GO TO 105
   25  X=A1**2-A2**2
       Y=-(A1**2)+3.0*A2**2-2.0*A3**2
       Z=A1**2-A2**2+A3**2
       GO TO 105
   35  X=A1**2-2.0*A2**2+A3**2
       Y=A1**2-A3**2
       Z=A1**2-A2**2+A3**2
       GO TO 105
   45  X=-(A2**2)+A3**2
       Y=-2.0*A1**2+3.0*A2**2-A3**2
       Z=A1**2-A2**2+A3**2
       GO TO 105
   55  X=-(A1**2)+A2**2
       Y=-(A1**2)+3.0*A2**2-2.0*A3**2
       Z=A1**2-A2**2+A3**2
       GO TO 105
   65  X=-(A1**2)+2.0*A2**2-A3**2
       Y=-(A1**2)+A3**2
       Z=A1**2-A2**2+A3**2
  105  RETURN
       END
```

```
      C
      C*****************************************************************
      C
      C     THIS SUBROUTINE CALCULATES THE FIRST AND SECOND
      C     DIFFERENTIALS OF THE FUNCTIONS AC,BC,AND CD WITH
      C     RESPECT TO THE THREE CHOSEN MEAN EFFECTIVE COOLING
      C     VELOCITIES.
      C
      C*****************************************************************
      C
            SUBROUTINE CDABC(A1,B1,C1,A21,B21,C21,A2,B2,C2,A22,B22,C22,
           *A3,B3,C3,A23,B23,C23,X,Y,Z,K)
            IF(K.EQ.1) GO TO 16
            IF(K.EQ.2) GO TO 26
            IF(K.EQ.3) GO TO 36
            IF(K.EQ.4) GO TO 46
            IF(K.EQ.5) GO TO 56
            IF(K.EQ.6) GO TO 66
       16   A1=0.0
            B1=-4*X
            C1=2*X
            A21=0.0
            B21=-4.0
            C21=2.0
            A2=2.0*Y
            B2=6.0*Y
            C2=-2.0*Y
            A22=2.0
            B22=6.0
            C22=-2.0
            A3=-2.0*Z
            B3=-2.0*Z
            C3=2.0*Z
            A23=-2.0
            B23=-2.0
            C23=2.0
            GO TO 106
       26   A1=2.0*X
            B1=-2.0*X
            C1=2.0*X
            A21=2.0
            B21=-2.0
            C21=2.0
            A2=-2.0*Y
            B2=6.0*Y
            C2=-2.0*Y
            A22=-2.0
            B22=6.0
            C22=-2.0
            A3=0.0
            B3=-4.0*Z
            C3=2.0*Z
            A23=0
            B23=-4.0
            C23=2.0
            GO TO 106
       36   A1=2.0*X
```

```
      B1=2.0
      C1=2.0*X
      A21=2.0
      B21=2.0
      C21=2.0
      A2=-4.0*Y
      B2=0.0
      C2=-2.0*Y
      A22=-4.0
      B22=0.0
      C22=-2.0
      A3=2.0*Z
      B3=-2.0*Z
      C3=2.0*Z
      A23=2.0
      B23=-2.0
      C23=2.0
      GO TO 106
   46 A1=0.0
      B1=-4.0*X
      C1=2.0*X
      A21=0.0
      B21=-4.0
      C21=2.0
      A2=-2.0*Y
      B2=6.0*Y
      C2=-2.0*Y
      A22=-2.0
      B22=6.0
      C22=-2.0
      A3=2.0*Z
      B3=-2.0*Z
      C3=2.0*Z
      A23=2.0
      B23=-2.0
      C23=2.0
      GO TO 106
   56 A1=-2.0*X
      B1=-2.0*X
      C1=2.0*X
      A21=-2.0
      B21=-2.0
      C21=2.0
      A2=2.0*Y
      B2=6.0*Y
      C2=-2.0*Y
      A22=2.0
      B22=6.0
      C22=-2.0
      A3=0.0
      B3=-4.0*Z
      C3=2.0*Z
      A23=0.0
      B23=-4.0
      C23=2.0
      GO TO 106
   66 A1=-2.0*X
      B1=-2.0*X
      C1=2.0*X
      A21=-2.0
      B21=-2.0
      C21=2.0
      A2=4.0*Y
      B2=0.0
      C2=-2.0*Y
      A22=4.0
```

```
      B22=0.0
      C22=-2.0
      A3=-2.0*Z
      B3=2.0*Z
      C3=2.0*Z
      A23=-2.0
      B23=2.0
      C23=2.0
  106 RETURN
      END
C*************************************************************************
C
C     THIS SUBROUTINE CALCULATES THE COVARIANCES BETWEEN THE
C     VELOCITY FLUCTUATIONS USING A METHOD SUGGESTED BY KING.
C
C*************************************************************************
      SUBROUTINE COVAR(CV,V,N,IP,ZP,ZQ,ZR,AKPQ,AKPR,AKQP,AKQR,AKRP
     *,AKRQ,EITA)
      DIMENSION CV(50),V(50)
      EITA=0.5
      DO 15 I=1,6
      CV(I+6)=CV(I)
      V(I+6)=V(I)
   15 CONTINUE
      IF(V(IP).LE.0.002) GO TO 108
      ZETA1=SQRT(ZP**2-2.0*ZQ**2+2.0*ZR**2)
      ZETA3=SQRT(2.0*ZP**2-2.0*ZQ**2+ZR**2)
      PI1=CV(IP+3)-ZETA1-0.5*((1/CV(IP+3)-ZP**2/CV(IP+3)**3)*V(IP)
     *-(4.0*ZQ**2/CV(IP+3)**3+2.0/CV(IP+3))*V(IP+1)+(-4.0*ZR**2
     */CV(IP+3)**3+2.0/CV(IP+3))*V(IP+2))
      PI3=CV(IP+5)-ZETA3-0.5*((2.0/CV(IP+5)-4.0*ZP**2/CV(IP+5)**3
     *)*V(IP)+(-2.0/CV(IP+5)-4.0*ZQ**2/CV(IP+5)**3)*V(IP+1)+(1/CV(
     *IP+5)-ZR**2/CV(IP+5)**3)*V(IP+2))
      A1=-2.0*ZP**2*EITA/V(IP+1)
      B1=6.0*ZP*ZQ-(ZP*EITA/(ZQ*V(IP+1)))*(PI1*CV(IP+3)**3-PI3*CV
     *(IP+5)**3)
      C1=PI1*CV(IP+3)**3-2.0*PI3*CV(IP+5)**3
      IF(B1**2-4.0*A1*C1.LT.0) GO TO 57
      AKPQ1=(-B1+SQRT(B1**2-4.0*A1*C1))/(2.0*A1)
      AKPQ2=(-B1-SQRT(B1**2-4.0*A1*C1))/(2.0*A1)
      RPQ1=AKPQ1/SQRT(V(IP)*V(IP+1))
      RPQ2=AKPQ2/SQRT(V(IP)*V(IP+1))
      IF(ABS(RPQ1).GT.1) GO TO 17
      GO TO 27
   17 IF(ABS(RPQ2).GT.1) GO TO 37
      AKPQ=AKPQ2
   27 AKPQ=AKPQ1
      GO TO 47
   37 AKPQ=0.9*SQRT(V(IP)*V(IP+1))
   47 AKQR=(2.0*CV(IP)*CV(IP+1)*KPQ+PI1*CV(IP+3)**3-PI3*CV(IP+5)
     ***3)/(2.0*CV(IP+1)*CV(IP+2))
      RQR=AKQR*SQRT(V(IP+1)*V(IP+2))
      IF(ABS(RQR).GT.1) AKQR=0.9*SQRT(V(IP+1)*V(IP+2))
      AKPR=EITA*AKPQ*AKQR/V(IP+1)
      GO TO 107
   57 AKPQ=0.9*SQRT(V(IP)*V(IP+1))
      AKQR=0.9*SQRT(V(IP+1)*V(IP+2))
      AKPR=EITA*AKPQ*AKQR/V(IP+1)
      GO TO 107
  108 AKPQ=0.0
      AKQR=0.0
      AKPR=0.0
  107 AKQP=AKPQ
      AKRQ=AKQR
      AKRP=AKPR
      RETURN
      END
```

2

VITA

Salim Iqbal Janjua

Candidate for the Degree of

Master of Science

Thesis: TURBULENCE MEASUREMENTS IN A COMPLEX FLOWFIELD USING A SIX-ORIENTATION HOT-WIRE PROBE TECHNIQUE

Major Field: Mechanical Engineering

Biographical:

Personal Data: Born in Rawalpindi, Pakistan, October 17, 1952, the son of Mr. and Mrs. M. Aslam Janjua.

Education: Graduated from Punjab University with a Bachelor of Science degree in Physics and Mathematics in 1971; received the Bachelor of Engineering degree from Concordia University at Montreal, Canada in May, 1980; completed requirements for the Master of Science degree at Oklahoma State University in December, 1981.

Professional Societies: Member of American Institute of Aeronautics and Astronautics.